

Multiple Uses of Correlation Filters for Biometrics

Prof. Vijayakumar Bhagavatula
kumar@ece.cmu.edu



Acknowledgments

- Dr. Abhijit Mahalanobis (Lockheed Martin)
- Prof. Marios Savvides (ECE/CyLab)
- Dr. Chunyan Xie
- Dr. Jason Thornton
- Dr. Krithika Venkataramani
- Dr. Pablo Hennings
- Vishnu Naresh Boddeti
- Jon Smereka

- Many of the slides in this tutorial courtesy of Prof. Marios Savvides



Outline

- Example of correlation pattern recognition
- Matched filters
- Composite correlation filters
- Correlation filter applications in biometrics
 - Face recognition
 - Eye detection
 - Iris recognition
 - Ocular recognition
 - Cancellable biometric filters
 - Biometric encryption
- Summary

Correlation Pattern Recognition

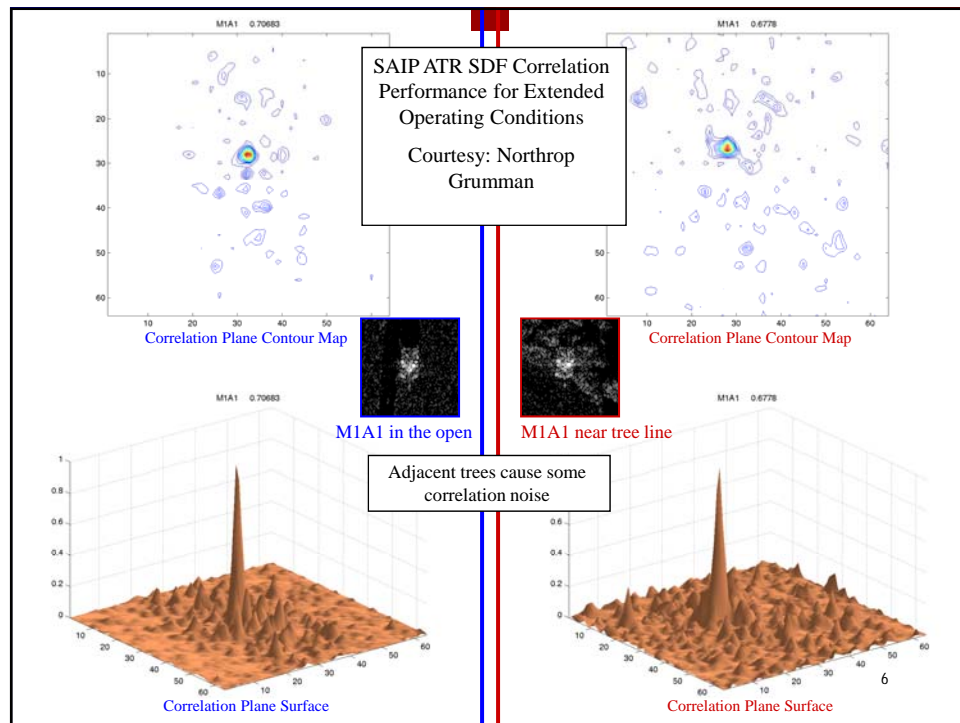
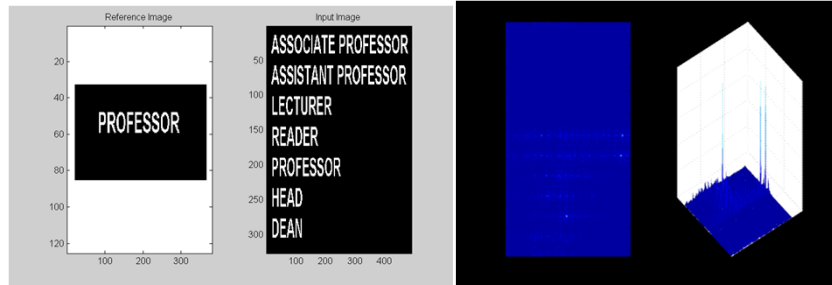
$$c(\tau_x, \tau_y) = \iint r(x, y) s(x - \tau_x, y - \tau_y) dx dy$$

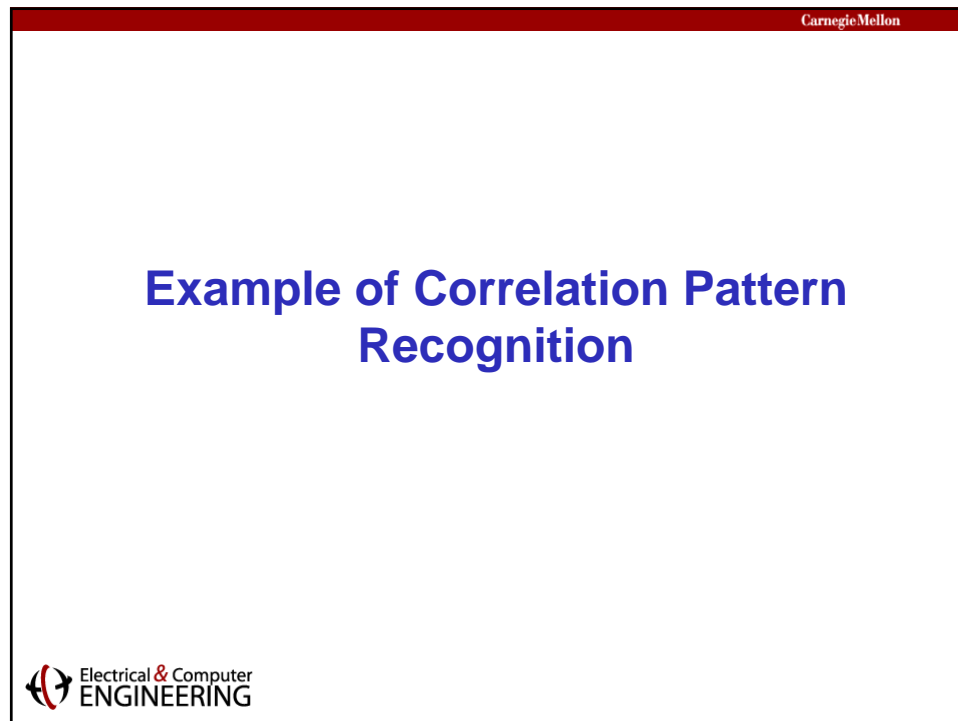
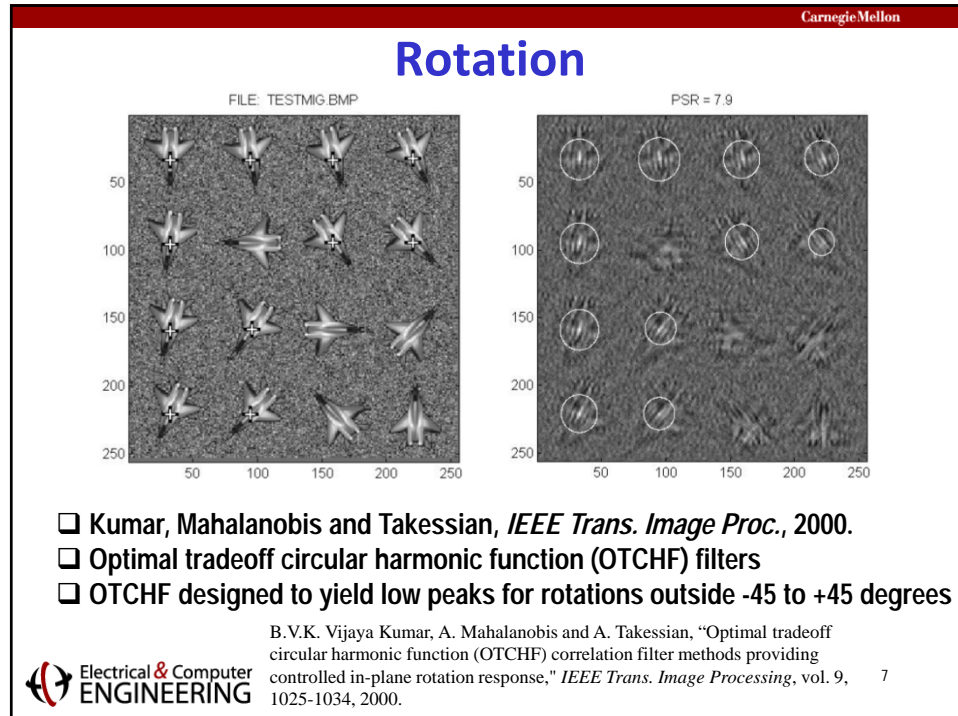
- Determine the cross-correlation between a carefully designed template $r(x,y)$ and test image $s(x,y)$ for **all possible shifts**.
- When the test image is authentic, correlation output exhibits a peak.
- If the test image is of an impostor, the correlation output will be low.
- Simple matched filters won't work well in practice, due to rotations, scale changes and other differences between test and reference images.
- Advanced distortion-tolerant correlation filters developed previously for automatic target recognition (ATR) applications, now being adapted for biometric recognition.

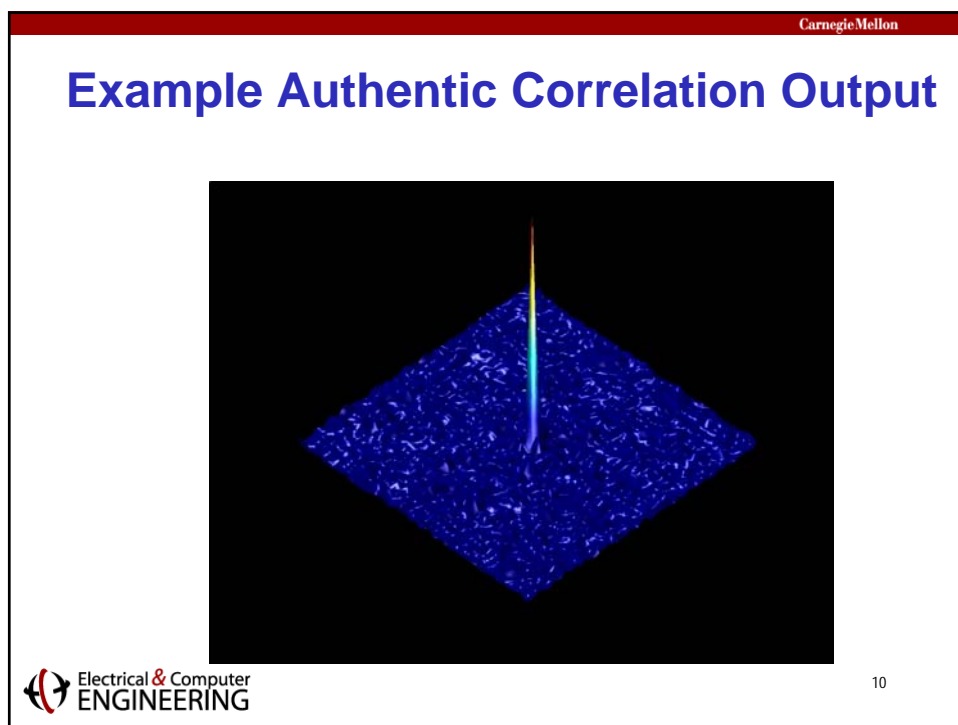
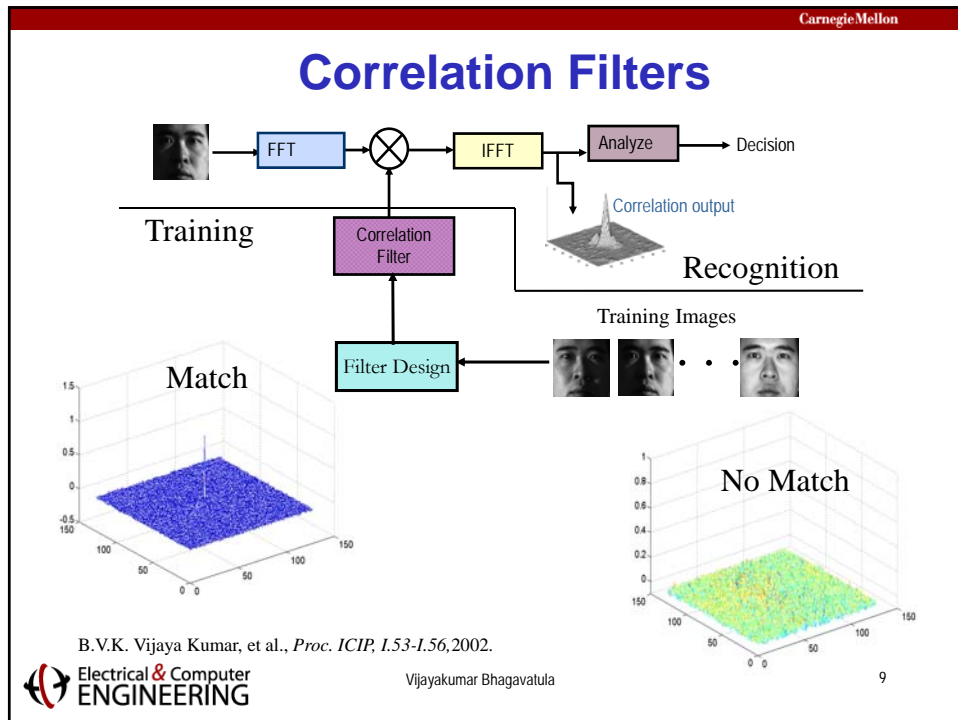
B.V.K. Vijaya Kumar, A. Mahalanobis and R. Juday, *Correlation Pattern Recognition*, Cambridge University Press, UK, November 2005.

Shift-Invariance

- Desired pattern can be anywhere in the input scene.
- Simple matched filters unacceptably sensitive to rotations, scale changes, etc.

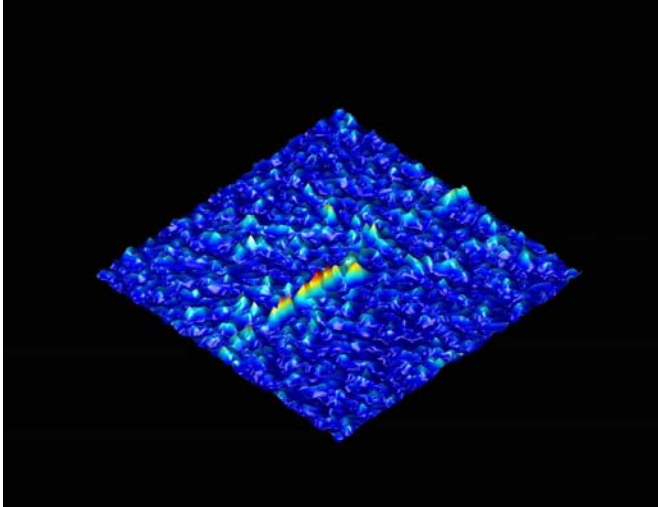






Carnegie Mellon

Example Impostor Correlation Output



 Electrical & Computer
ENGINEERING

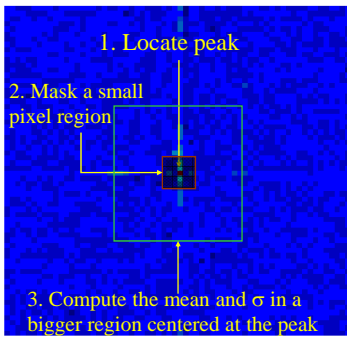
Vijayakumar Bhagavatula

11

Carnegie Mellon

Peak to Sidelobe Ratio (PSR)

- PSR invariant to constant illumination changes



$$PSR = \frac{Peak - mean}{\sigma}$$

- Match declared when PSR is large, i.e., peak must not only be large, but sidelobes must be small.

 Electrical & Computer
ENGINEERING

12

Carnegie Mellon

CMU PIE Database

13 cameras

21 Flashes

 Electrical & Computer
ENGINEERING

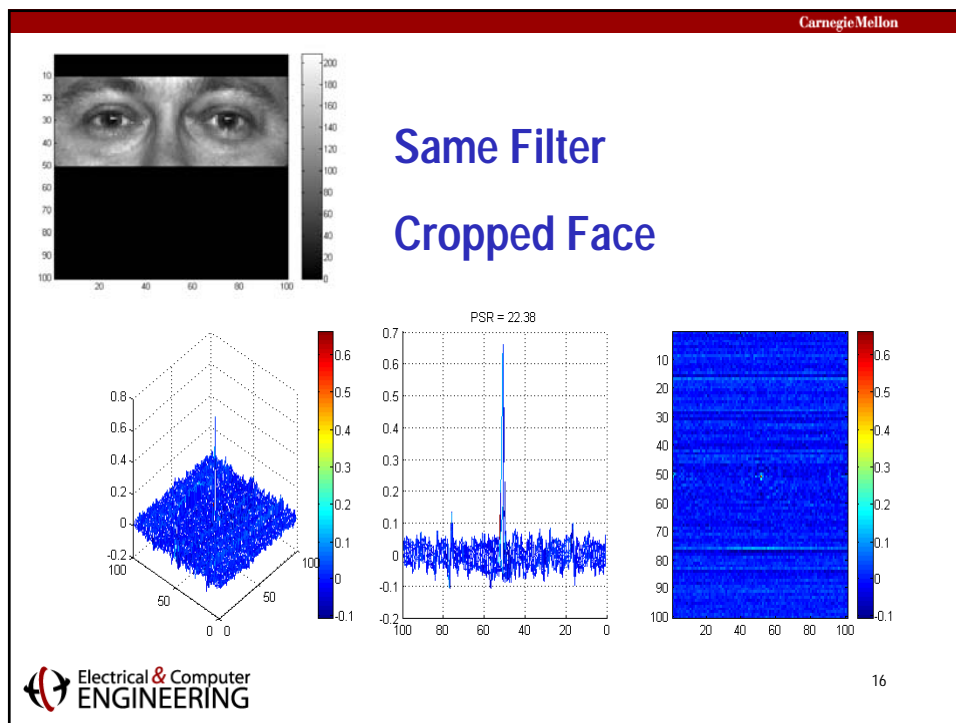
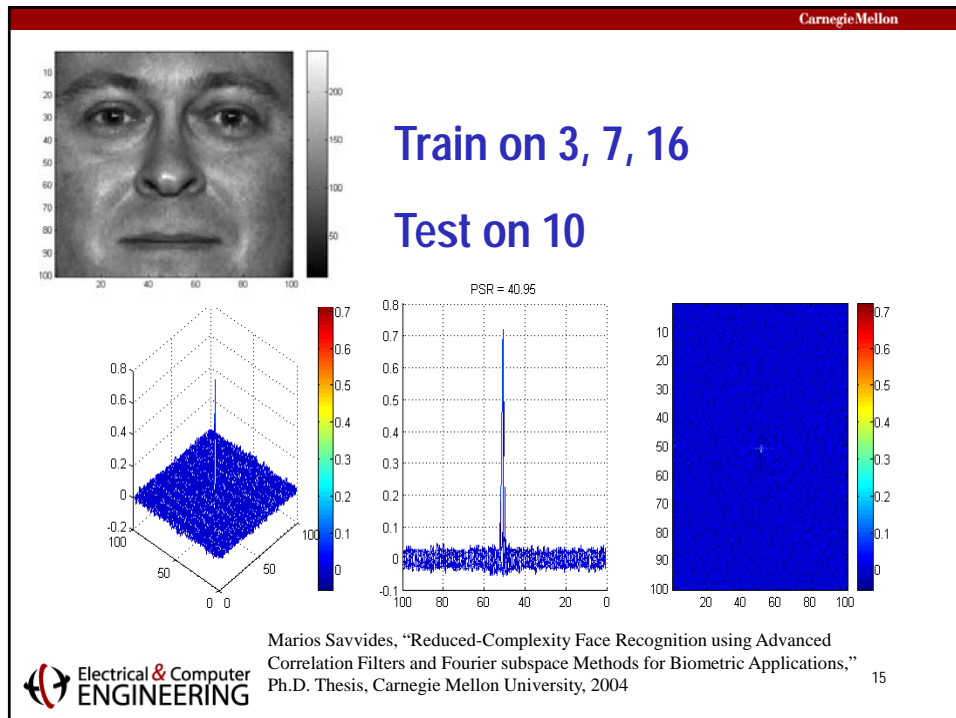
13

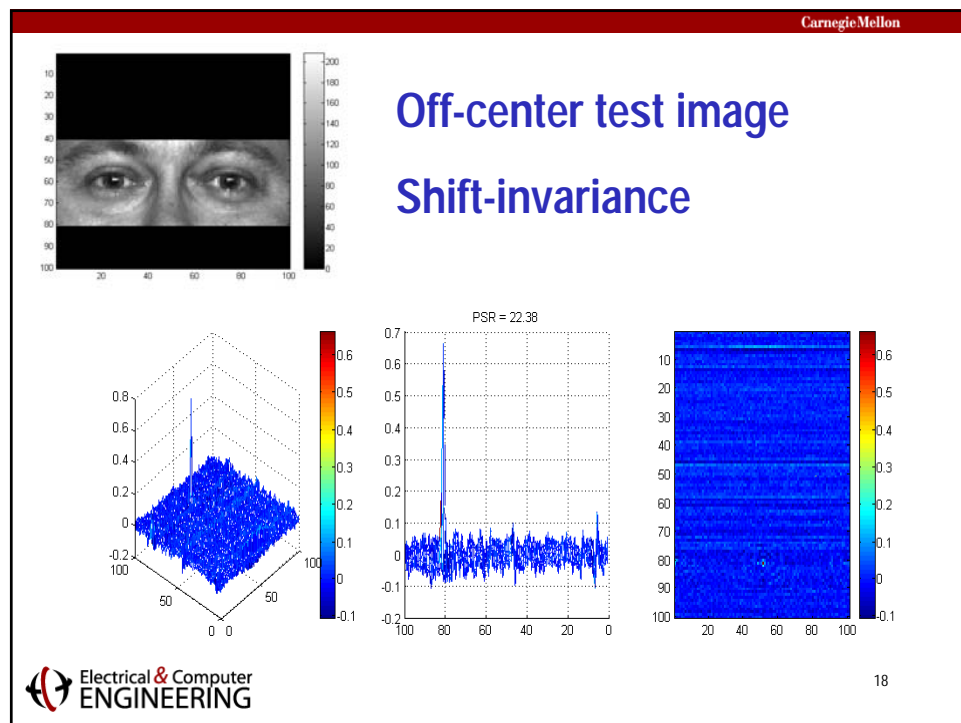
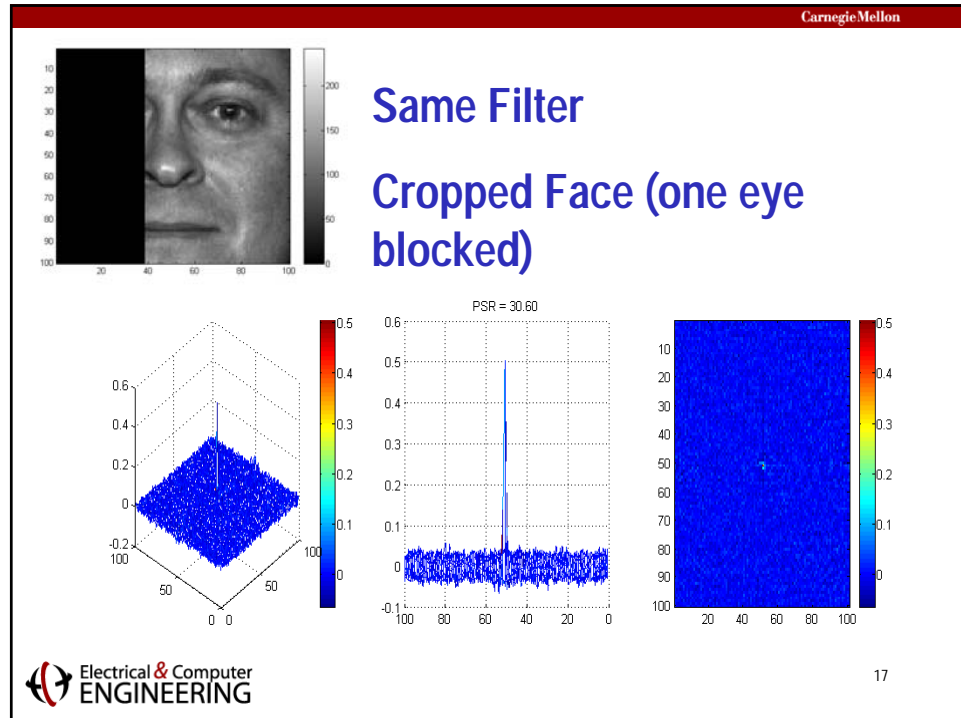
Carnegie Mellon

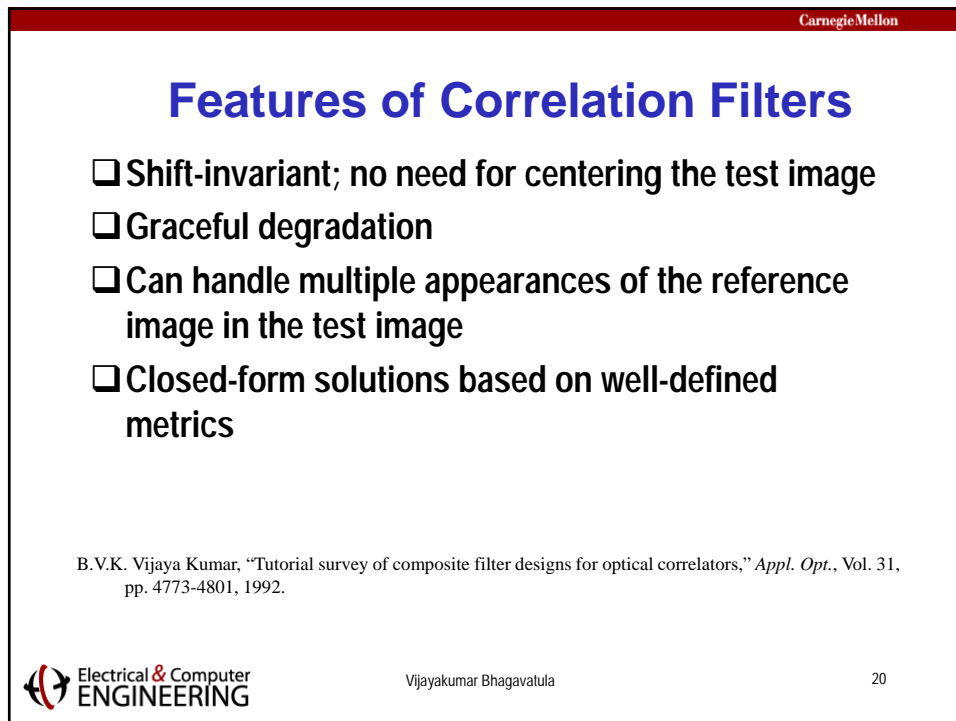
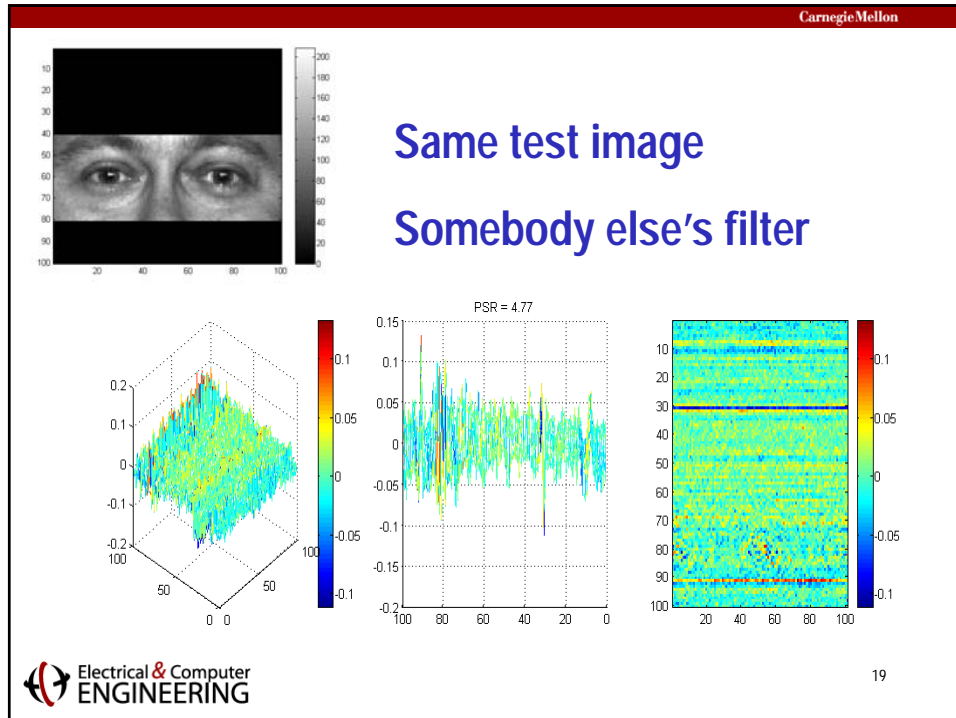
One Face, 21 Illuminations

 Electrical & Computer
ENGINEERING

14





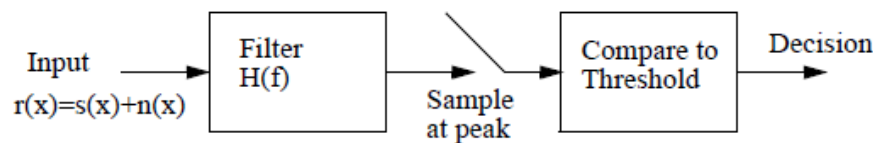


Matched Filters



Target Detection

- ❑ Developed for optimal detection of radar returns
- ❑ Received signal $r(\cdot)$ is either just noise (i.e., no target) or reflected signal + noise (i.e., target present)
- ❑ Received signal input to a filter with frequency response $H(f)$ and its output peak compared to a threshold to make the target decision
- ❑ What should $H(f)$ be?



Signal-to-Noise Ratio (SNR)

- Filter peak output in the absence of noise is

$$y_p = \int S(f)H(f)df$$

- Output variance due to input additive noise is

$$\sigma^2 = \int P_n(f)|H(f)|^2 df$$

- Signal-to-noise ratio (SNR) is the ratio of peak intensity to noise variance

$$SNR = \frac{|y_p|^2}{\sigma^2} = \frac{\left| \int S(f)H(f)df \right|^2}{\int P_n(f)|H(f)|^2 df}$$

- To find filter H(f) that maximizes SNR, we use Cauchy-Schwartz inequality

$$\left| \int A(f)B(f)df \right|^2 \leq \int |A(f)|^2 df \int |B(f)|^2 df$$

with equality if and only if $A(f) = \alpha B^*(f)$ with α an arbitrary constant.

Optimal Filter

- Let us try following choices for A(f) and B(f)

$$A(f) = \frac{S(f)}{\sqrt{P_n(f)}} \text{ and } B(f) = H(f)\sqrt{P_n(f)}$$

- Then SNR is upperbounded as follows

$$SNR = \frac{\left| \int \frac{S(f)}{\sqrt{P_n(f)}} H(f) \sqrt{P_n(f)} df \right|^2}{\int P_n(f) |H(f)|^2 df} \leq \frac{\left(\int \frac{|S(f)|^2}{P_n(f)} df \right) \left(\int P_n(f) |H(f)|^2 df \right)}{\int P_n(f) |H(f)|^2 df} = \frac{\left(\int \frac{|S(f)|^2}{P_n(f)} df \right)}{\int P_n(f) |H(f)|^2 df} = SNR_{MAX}$$

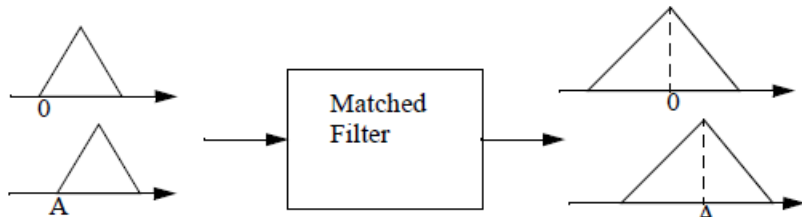
with equality if and only if $H(f) = \alpha \frac{S^*(f)}{P_n(f)}$

Matched Filter

- ❑ If the noise is white, its power spectral density is a constant, i.e., $P_n(f) = N_0$.
- ❑ Optimal filter $H(f)$ is proportional to $S^*(f)$, the complex conjugate of the Fourier transform (FT) of the transmitted signal $s(t)$
- ❑ Optimal filter's magnitude matches the magnitude of the reference signal FT, hence **matched** filter
- ❑ Optimal filter's phase is exactly negative of the phase of the reference signal FT

Matched Filter Output Peak

- ❑ If the test signal is identical to the reference signal $s(t)$, matched filter output peak occurs at the origin
- ❑ If the test signal is $s(t-A)$, the output peak occurs at A , i.e., Output peak location gives the input location



Cross-Correlation

- ❑ Test signal $r(t)$
- ❑ Filter $H(f) = S^*(f)$, matched to reference signal $s(t)$
- ❑ Matched filter output $y(\cdot)$ is the cross-correlation of $r(t)$ and $s(t)$
- ❑ If $r(t) = s(t)$, output is the autocorrelation function
- ❑ Autocorrelation larger than cross-correlation
- ❑ Easily extended to images and higher dimensions

$$\begin{aligned}y(x) &= \text{IFT}\{R(f)H(f)\} = \text{IFT}\{R(f)S^*(f)\} \\&= \text{conv}\{r(t), s(-t)\} = \int r(t)s(t+x)dt\end{aligned}$$

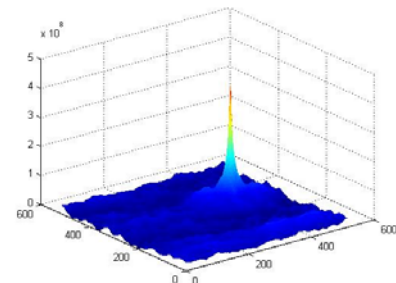
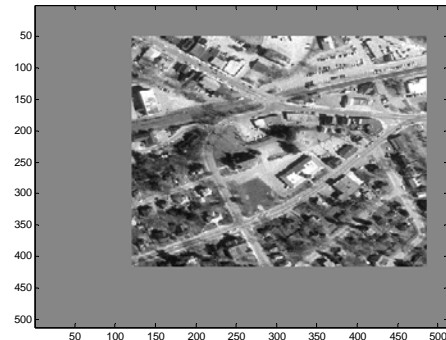
Power of Cross-Correlation



366x364 Reference Image

Carnegie Mellon

Test Scene

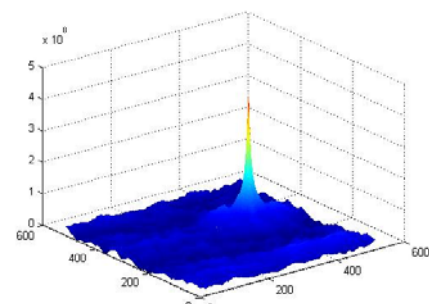
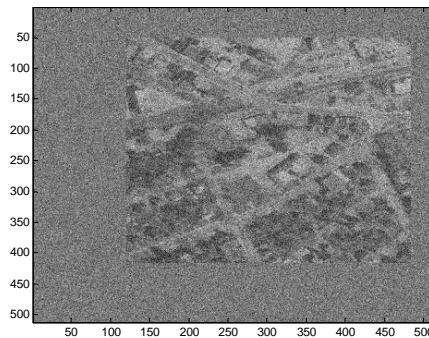


Vijayakumar Bhagavatula

29

Carnegie Mellon

Noisy Test Scene

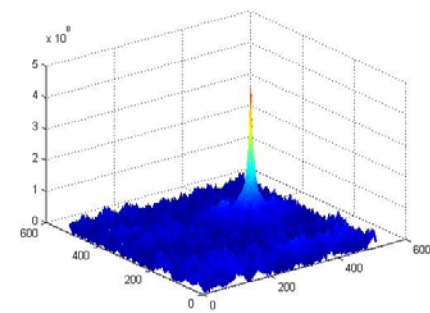
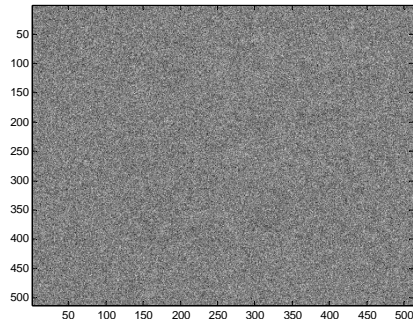


Vijayakumar Bhagavatula

30

Carnegie Mellon

Very Noisy Test Scene

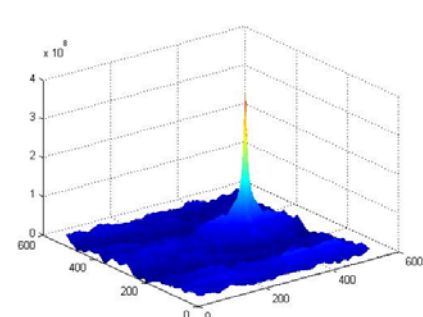
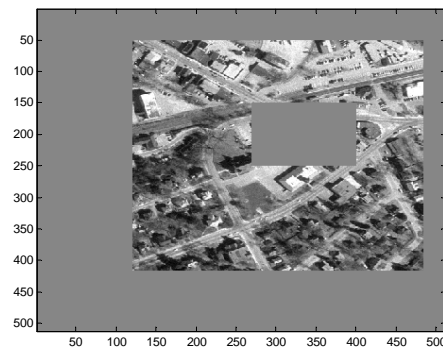


Vijayakumar Bhagavatula

31

Carnegie Mellon

Occluded Test Scene

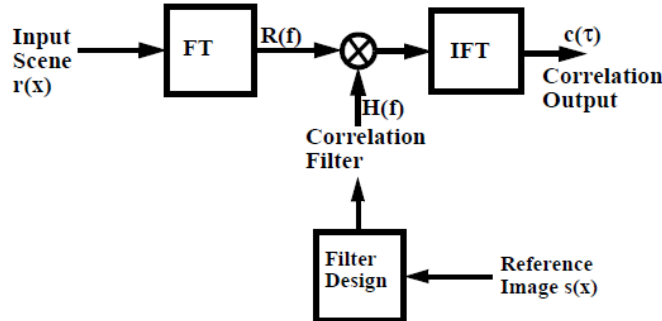


Vijayakumar Bhagavatula

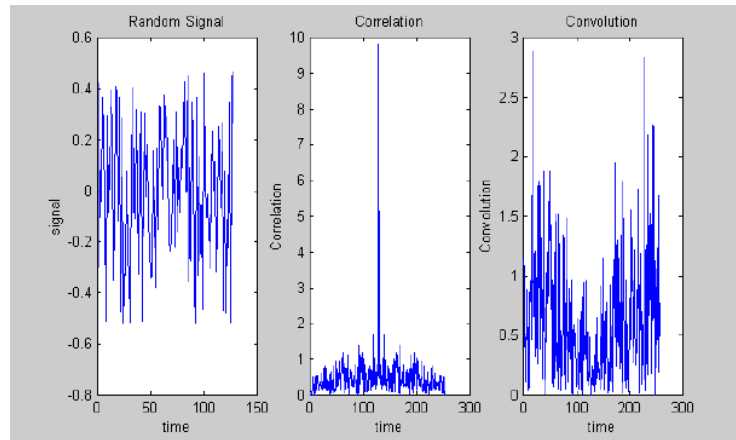
32

Cross-Correlation via FFTs

- ❑ Cross-correlation implemented efficiently via fast Fourier transform (FFT)
- ❑ For every test image, need two FFTs



Convolution vs. Correlation



- ❑ Convolution useful for filtering
- ❑ Correlation useful for matching

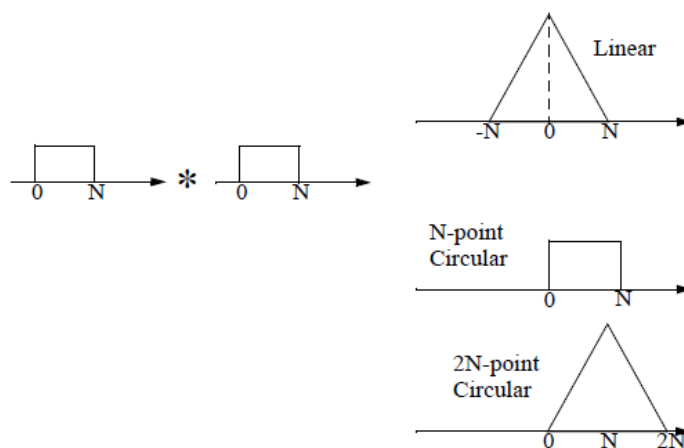
Circular Correlation

- ❑ When using N-point FFTs, we get N-point circular correlation rather than linear correlation
- ❑ Circular correlation is an aliased version of linear correlation

$$C_N[k] = \sum C[k - iN]$$

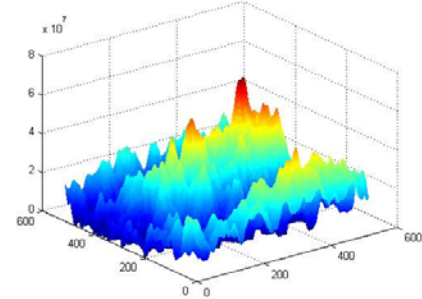
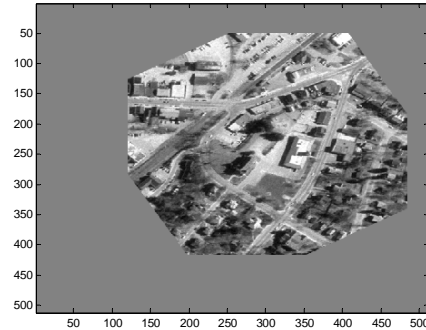
- ❑ To avoid circular correlation, we pad the two signals/images with zeros and use sufficiently large FFTs.

Linear vs. Circular Correlation



Sensitivity to Rotation

- ❑ Reference image rotated counter clockwise by 30 degrees



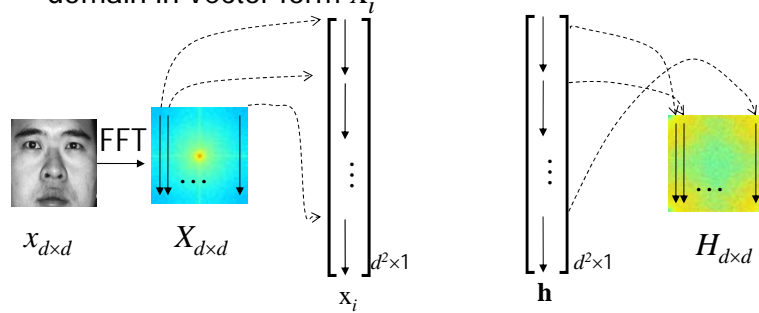
Composite Correlation Filters

Composite Correlation Filters

- ❑ Matched filter (MF) overly sensitive to rotations and scale changes
- ❑ In principle, we can design one MF for each rotated view, but the number of filters will become impractically large
- ❑ Composite filters (also known as synthetic discriminant function or SDF filters) designed to provide improved tolerance to distortions (e.g., rotations, scale changes, etc.)
- ❑ Filters designed from training sets containing distorted views of the reference target

Vector Representation

- An image in the frequency domain in vector form x_i
- Filter h



- N images

$$\mathbf{X}_{d^2 \times N} = [\mathbf{x}_1, \mathbf{x}_2, \dots, \mathbf{x}_N]$$

Correlation Peak

- ❑ For MF, the correlation peak is guaranteed to occur at the origin when the query is the centered reference image
- ❑ When the test image is a shifted version of the reference, the correlation peak location indicates the shift
- ❑ $X(u,v)$ is the 2-D discrete Fourier transform (DFT) of the image $x(m,n)$
- ❑ SDF filters constrain the correlation values at the origin (loosely called peaks) for centered training images

$$c(0,0) = \sum_{i=0}^{d-1} \sum_{j=0}^{d-1} h(i,j) x(i,j) = \sum_{u=0}^{d-1} \sum_{v=0}^{d-1} H(u,v) X(u,v) = \mathbf{h}^T \mathbf{x}$$

Equal Correlation Peak (ECP) SDF

- ❑ First SDF filter (Hester & Casasent, *Applied Optics*, 1980)
 - ❑ Filter \mathbf{h} is assumed to be a weighted sum of training image FTs, i.e.,
- $$\mathbf{h} = a_1 \mathbf{x}_1 + a_2 \mathbf{x}_2 + \cdots + a_N \mathbf{x}_N \quad \mathbf{h} = \mathbf{X}\mathbf{a} \text{ where } \mathbf{a} = [a_1 \ a_2 \ \cdots \ a_N]^T$$
- ❑ Weights chosen so that the correlation output (at the origin) equals a pre-specified value (e.g., 1 for authentic images and 0 for impostor images) for training images

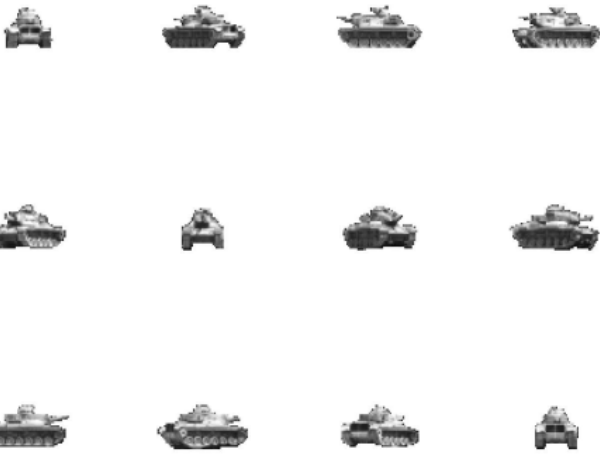
$$\mathbf{x}_i^T \mathbf{h} = c_i \text{ for } i = 1, 2, \dots, N \Rightarrow \mathbf{X}^T \mathbf{h} = \mathbf{c}$$

- ❑ This leads to the following solution for filter vector

$$\mathbf{X}^T (\mathbf{X}\mathbf{a}) = \mathbf{c} \Rightarrow \mathbf{a} = (\mathbf{X}^T \mathbf{X})^{-1} \mathbf{c} \Rightarrow \mathbf{h} = \mathbf{X}\mathbf{a} = \mathbf{X}(\mathbf{X}^T \mathbf{X})^{-1} \mathbf{c}$$

Carnegie Mellon

Database for (ECP) SDF



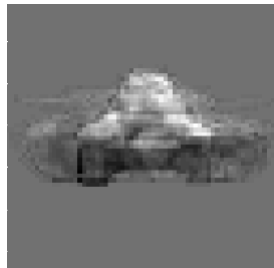
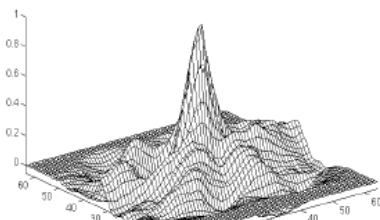
 Electrical & Computer
ENGINEERING

Vijayakumar Bhagavatula

43

Carnegie Mellon

(ECP) SDF Template

- ❑ Correlation peak is not very sharp making localization inaccurate
- ❑ Filter controls only one value in the correlation outputs
- ❑ Sidelobes can be larger than the controlled value

 Electrical & Computer
ENGINEERING

Vijayakumar Bhagavatula

44

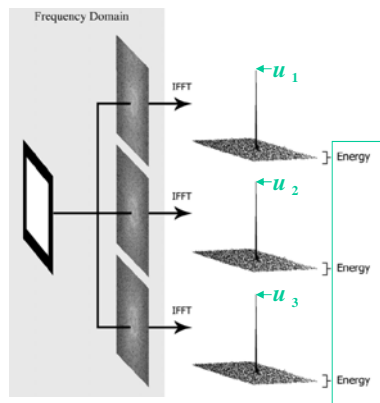
Correlation Plane Energy

- ❑ Sharp correlation peaks enable accurate localization of the target in the test scene (e.g., the task of locating eyes in a face image)
- ❑ Sharp peaks can be obtained by minimizing the correlation plane energy while constraining the correlation peak (at the origin) to 1
- ❑ Correlation plane energy can be expressed as follows

$$E = \sum_i \sum_j |c(i, j)|^2 = \sum_u \sum_v |C(u, v)|^2 = \sum_u \sum_v |H(u, v)|^2 |X(u, v)|^2 = \mathbf{h}^+ \mathbf{D} \mathbf{h}$$

where $\mathbf{D}_{d^2 \times d^2} = \text{Diag} \left\{ |X(1,1)|^2 \quad |X(1,2)|^2 \quad \dots \quad |X(d,d)|^2 \right\}$

Minimum Average Correlation Energy (MACE) Filter



$$\begin{aligned} ACE &= \hat{\mathbf{h}}^+ \hat{\mathbf{D}} \hat{\mathbf{h}} \\ \hat{\mathbf{x}}_i^+ \hat{\mathbf{h}} &= u_i \quad i = 1, \dots, N \\ \hat{\mathbf{D}}(k, k) &= \frac{1}{N} \sum_{i=1}^N |\hat{\mathbf{x}}_i(k)|^2 \end{aligned}$$

Minimum Average Correlation Energy (MACE) Filter

- Minimizing average correlation energy can be done directly in the frequency domain by averaging the correlation plane energies E_i as follows.

$$E_i = \sum_{u,v} |H(u,v)|^2 |X_i(u,v)|^2 = \mathbf{h}^+ \mathbf{X}_i \mathbf{X}_i^* \mathbf{h} = \mathbf{h}^+ \mathbf{D}_i \mathbf{h}$$

$$E_{ave} = \frac{1}{N} \sum_{i=1}^N E_i = \mathbf{h}^+ \left[\frac{1}{N} \sum_{i=1}^N \mathbf{X}_i \mathbf{X}_i^* \right] \mathbf{h} = \mathbf{h}^+ \mathbf{D} \mathbf{h}$$

$\mathbf{h} = \begin{bmatrix} X_i(1) \\ X_i(2) \\ X_i(3) \\ \vdots \\ X_i(d) \end{bmatrix}$

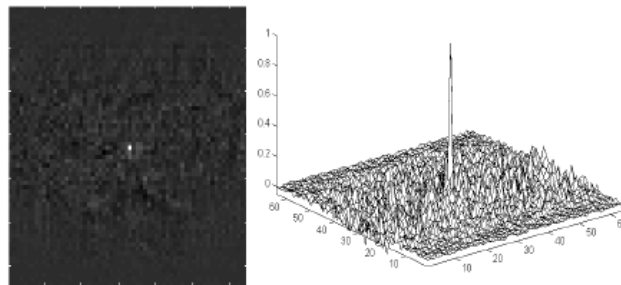
- Minimizing average correlation energy $\mathbf{h}^+ \mathbf{D} \mathbf{h}$ subject to the constraints $\mathbf{X}^+ \mathbf{h} = \mathbf{c}$ leads to the MACE filter solution

$$\mathbf{h} = \mathbf{D}^{-1} \mathbf{X} (\mathbf{X}^+ \mathbf{D}^{-1} \mathbf{X})^{-1} \mathbf{c}$$

A. Mahalanobis, B.V.K. Vijaya Kumar, and D. Casasent, "Minimum average correlation energy filters," *Appl. Opt.* 26, pp. 3633-3630, 1987.

MACE Filter Properties

- MACE filter produces sharp peaks leading to good localization and discrimination
- MACE filter emphasizes high spatial frequencies leading to noise sensitivity and poor generalization



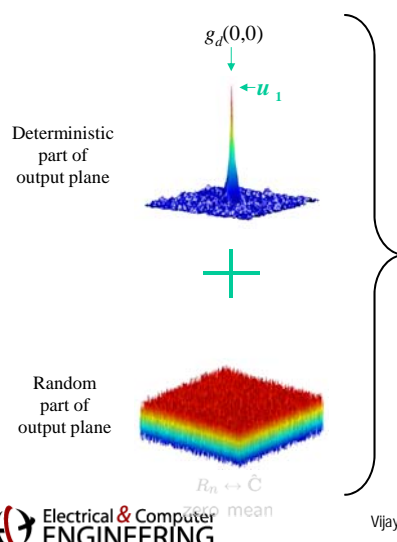
Output Noise Variance

- ❑ Input image corrupted by additive noise with power spectral density $P_n(u,v)$
- ❑ Correlation output will be corrupted by additive noise with power spectral density $P_n(u,v)|H(u,v)|^2$
- ❑ Output noise variance (ONV) given as follows

$$ONV = \sum_u \sum_v |H(u,v)|^2 P_n(u,v) = \mathbf{h}^T \mathbf{P} \mathbf{h}$$

where $\mathbf{P}_{d^2 \times d^2} = \text{Diag} \{ P_n(1,1) \quad P_n(1,2) \quad \dots \quad P_n(d,d) \}$

Minimum Variance Correlation Filter



- ❑ Minimum variance SDF produces filters that enhance low spatial frequencies and thus produce broad correlation peaks

B.V.K. Vijaya Kumar, "Minimum variance synthetic discriminant functions," *JOSA-A*, vol. 3, 1579-84, 1986

Optimal Trade-off SDF (OTSDF)

- ❑ MACE filter minimizes average correlation energy (ACE) while satisfying $X^T h = c$
- ❑ Minimum variance SDF (MVSDF) filter minimizes output noise variance (ONV) while satisfying $X^T h = c$
- ❑ MACE amplifies high frequencies whereas MVSDF amplifies low frequencies, i.e., the two goals conflict
- ❑ OTSDF is aimed minimizing one of the two criteria (e.g., ACE) while holding the other (e.g., ONV) constant and satisfying $X^T h = c$

$$h_{OTSDF} = T^{-1} X \left(X^T T^{-1} X \right)^{-1} c \quad \text{where } T = \alpha D + \sqrt{1 - \alpha^2} P, \quad 0 \leq \alpha \leq 1$$

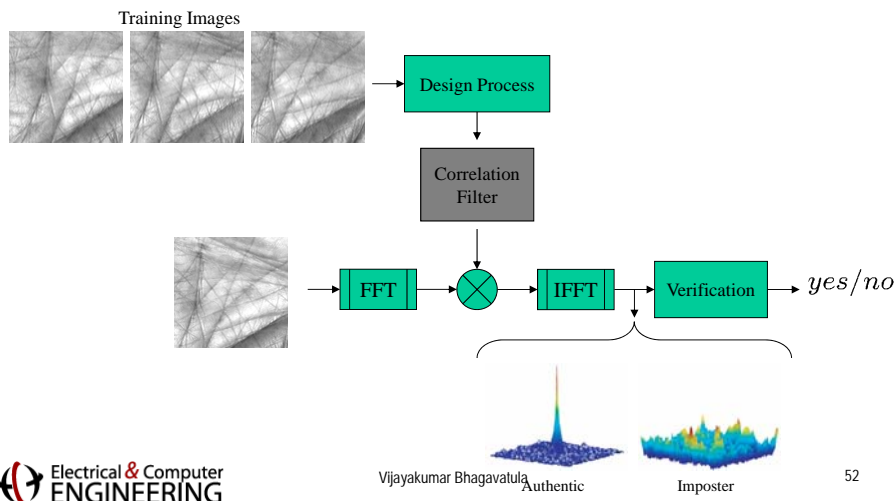
Ph. Refregier, "Filter Design For Optical Pattern Recognition: Multicriteria Optimization Approach," *Optics Letters*, Vol. 15, 854-856, 1990.

Vijayakumar Bhagavatula

51



Correlation Filters: Enrollment & Verification



Vijayakumar Bhagavatula

52

Brief Correlation Filter History

- First Synthetic Discriminant Function (SDF) filter (Hester and Casasent, 1980): a weighted sum of training images
- Generalized SDF (Bahri and Kumar, 1986): doesn't have to be a weighted sum of training images, better solutions available
- Minimum variance SDF (Kumar, 1986): minimum noise sensitivity
- Minimum average correlation energy (MACE) filters (Mahalanobis, Kumar and Casasent, 1987): minimize correlation energy leading to sharp correlation peaks
- Optimal tradeoff SDF (Refregier, 1992): optimal combinations of MVSDF and MACE filters
- Maximum average correlation height (MACH) filter (Mahalanobis, Kumar, Song, Sims and Epperson, 1994): relaxed peak constraints, filter design requires no matrix inversion

Brief Correlation Filter History (Cont'd.)

- Distance classifier correlation filter (DCCF) (Mahalanobis, Kumar and Sims, 1996): classification based on the entire correlation plane, not just the peak
- Polynomial correlation filter (PCF) (Mahalanobis and Kumar, 1997): Generalize correlation filters to include point nonlinearities
- Optimal trade-off circular harmonic function (OTCHF) filter (Kumar, Mahalanobis and Takessian, 2000): correlation filter with specified response to in-plane rotations
- Quadratic correlation filter (QCF) (Mahalanobis, Muise & Stanfill, 2004): shift-invariant quadratic correlation via a bank of linear filters
- Mellin radial harmonic transform (MRHT) filters (Kerekes and Kumar, 2006): correlation filter with controlled response to scale changes
- Max-margin correlation filters (MMCF) (Boddeti, Rodriguez, Kumar and Mahalanobis, 2011): combines CFs with support vector machines

Correlation Filters on Face Recognition Grand Challenge (FRGC) Data



Face Recognition Grand Challenge (FRGC): Expt. 4

- To facilitate the advancement of face recognition research, FRGC was organized by NIST
- Generic training set of 12,776 images from 222 subjects
- Gallery set of 16,028 controlled face images from 466 people
- Probe set of 8,014 uncontrolled face images from same 466 people
- Baseline principal components algorithm (PCA) yields a verification rate of 12% at 0.1% false accept rate (FAR)

P. J. Phillips, P. J. Flynn, T. Scruggs, K. W. Bowyer, J. Chang, K. Hoffman, J. Marques, J. Min, and W. Worek, "Overview of the Face Recognition Grand Challenge," *In Proceedings of IEEE Conference on Computer Vision and Pattern Recognition*, 2005



Carnegie Mellon

FRGC Gallery Images



Controlled (Indoor)

16,028 gallery images of 466 people

 Electrical & Computer
ENGINEERING

57

Carnegie Mellon

FRGC Probe Images

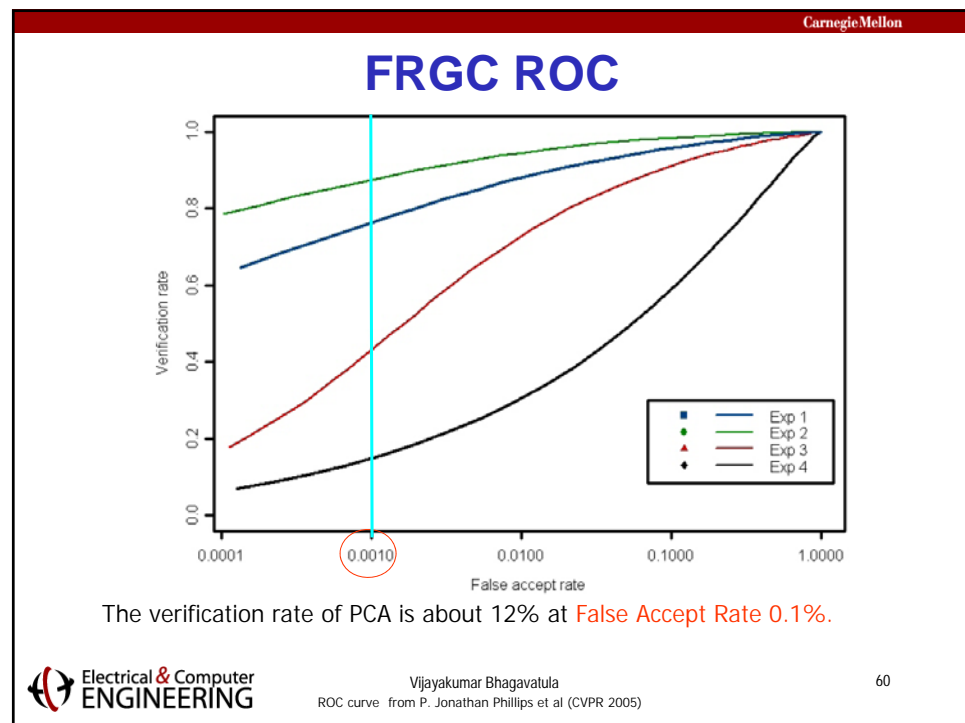
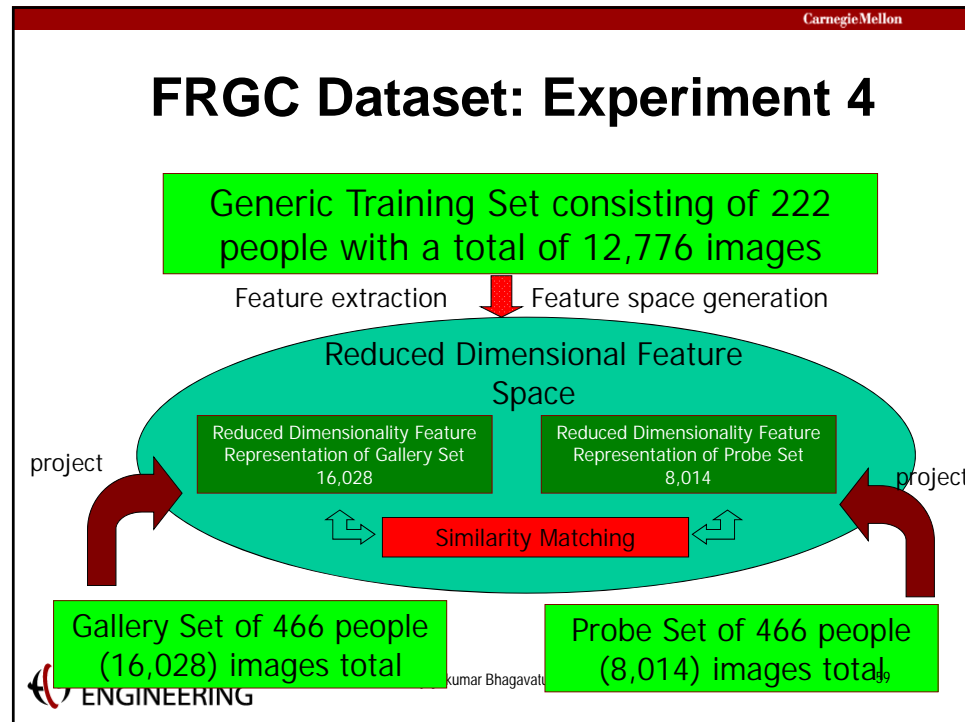


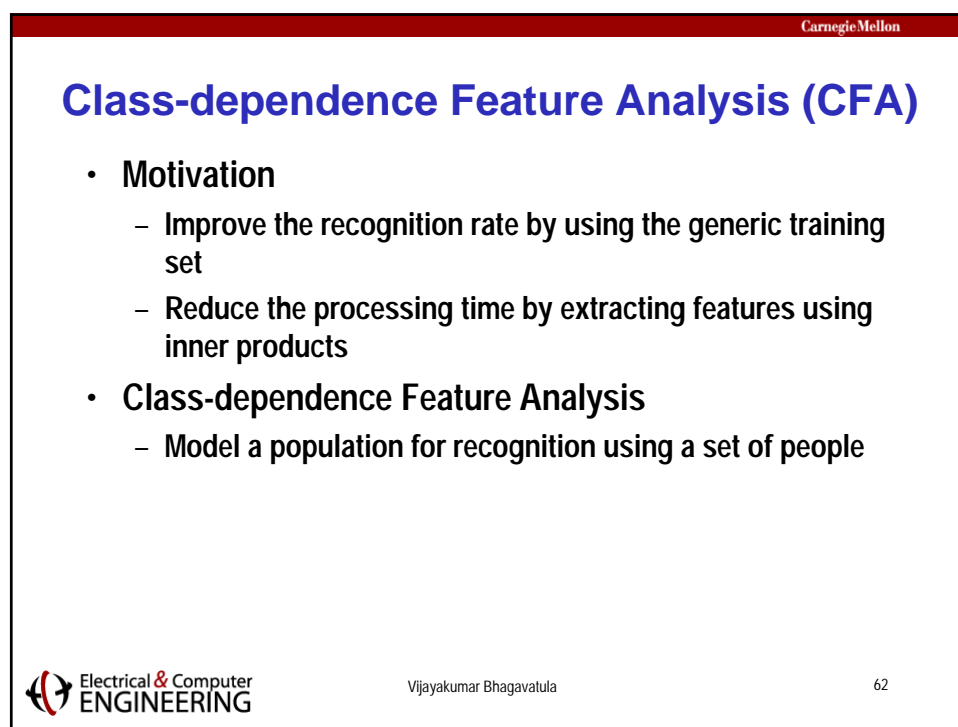
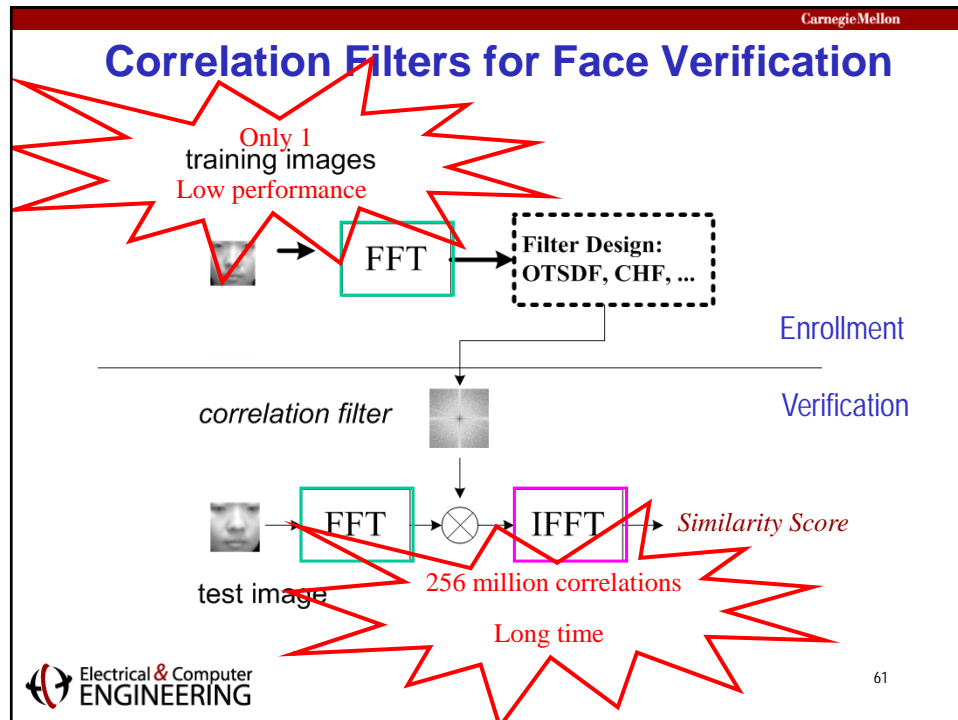
Uncontrolled (Indoor)

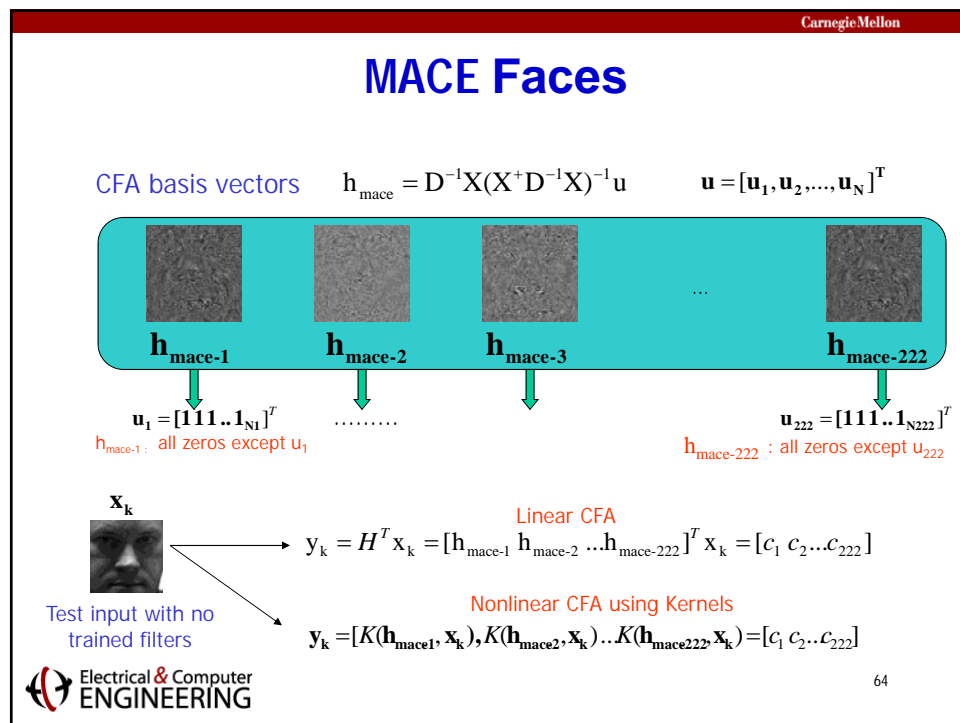
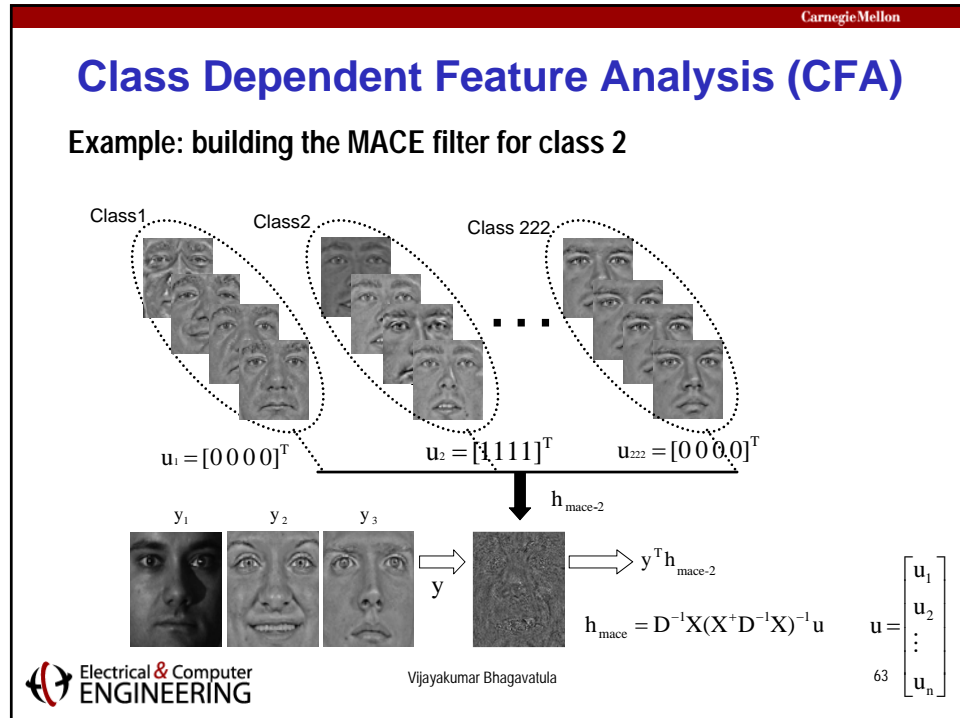
8,014 gallery images of 466 people

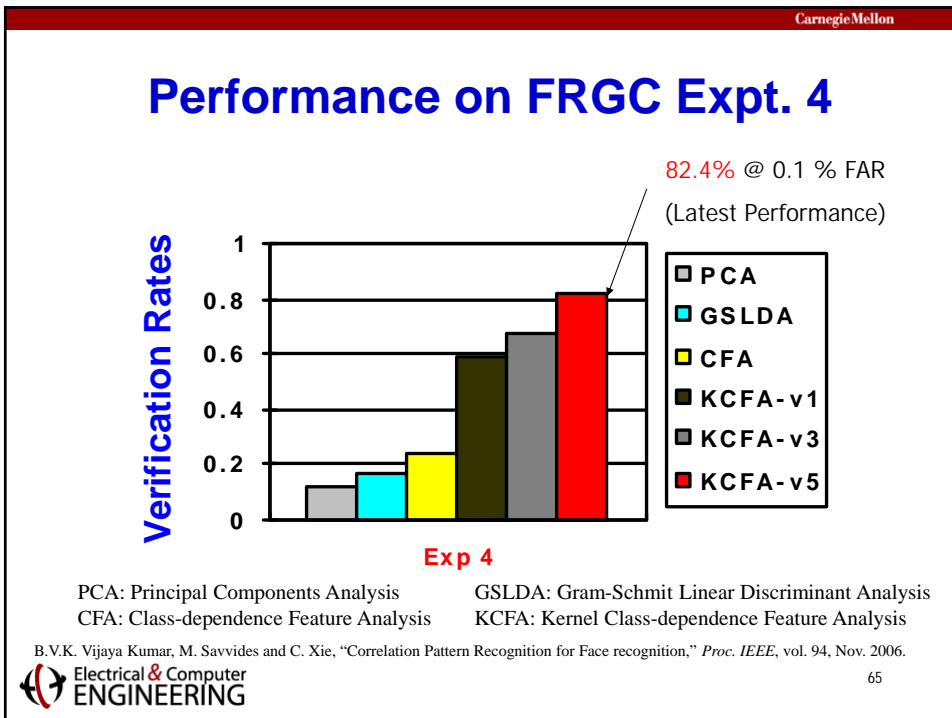
 Electrical & Computer
ENGINEERING

58



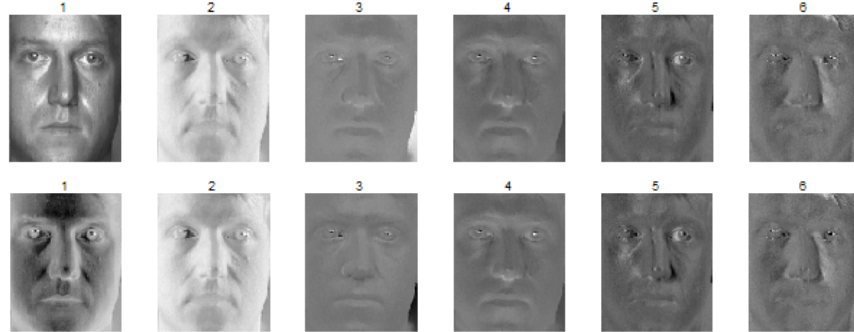




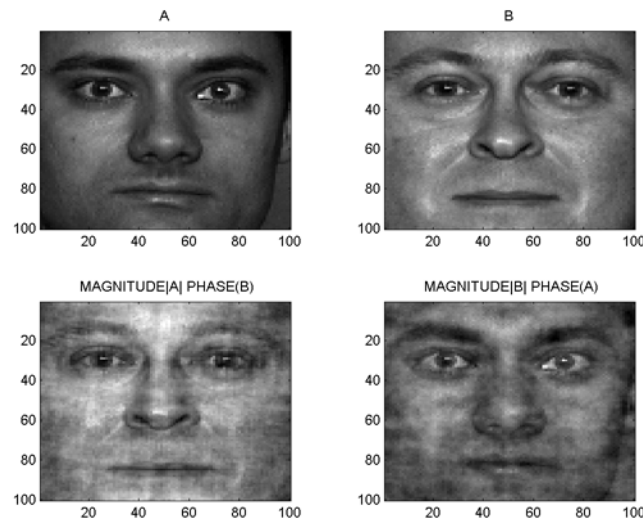


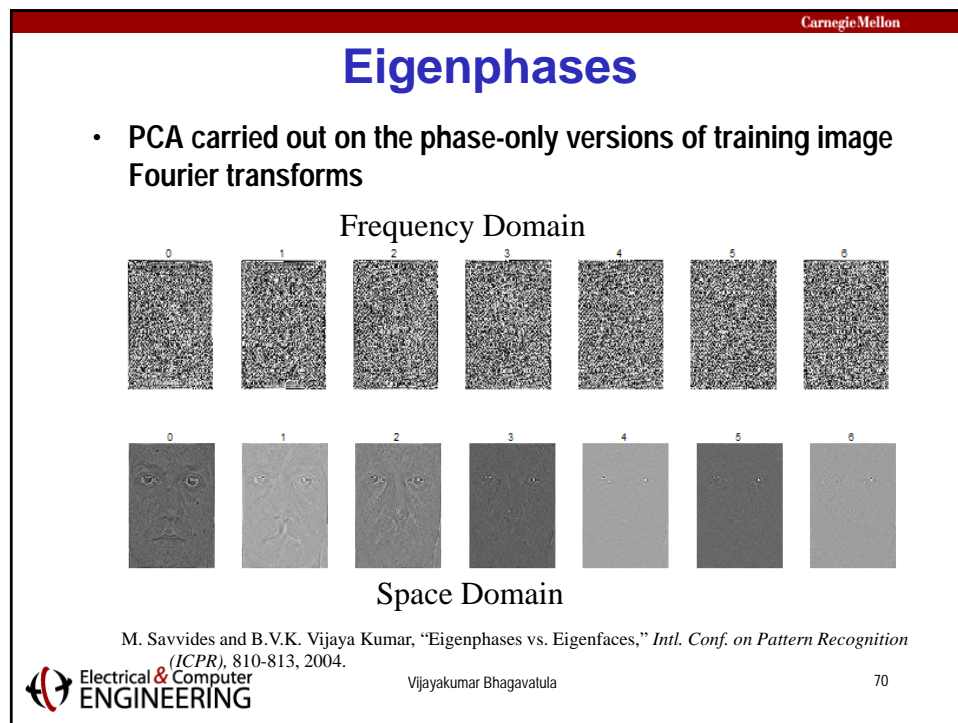
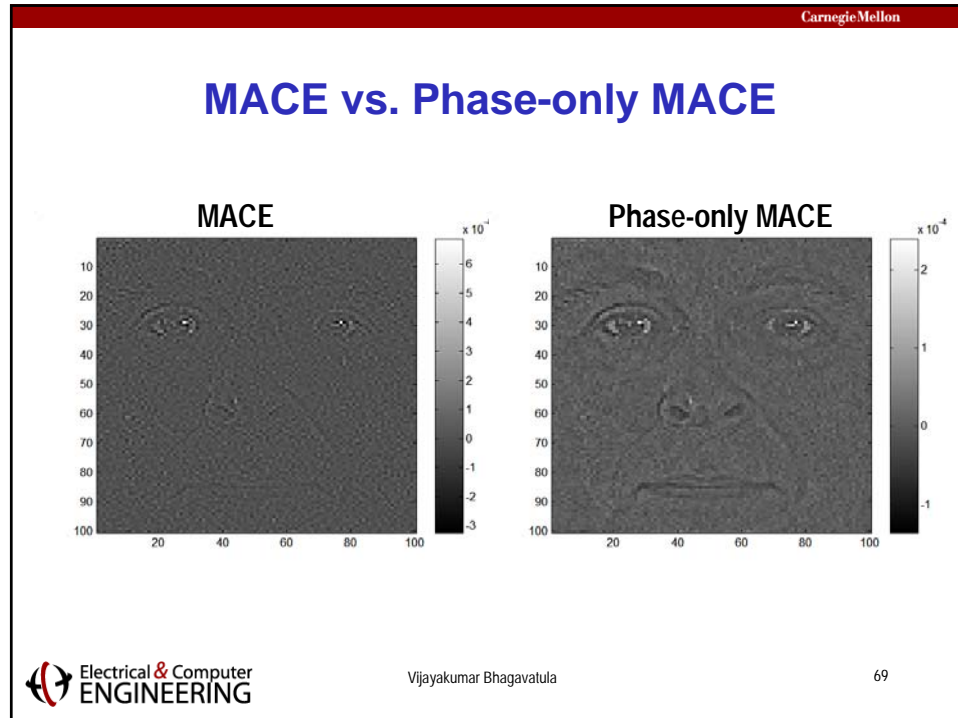
PCA in Frequency Domain

- Is there any advantage to carrying out PCA on the Fourier transforms of training images?
- Since FT is unitary, no differences (except for sign changes) in the eigenfaces obtained via space domain or frequency domain.



Importance of FT Phase





PIE Database Experiments

1	3,7,16	9	5-12
2	1,10,16	10	5-10
3	2,7,16	11	5,7,9,10
4	4,7,13	12	7,10,19
5	1,2,7,16	13	6,7,8
6	3,10,16	14	8,9,10
7	3,16,20	15	18,19,20
8	5-10,18,19,20		



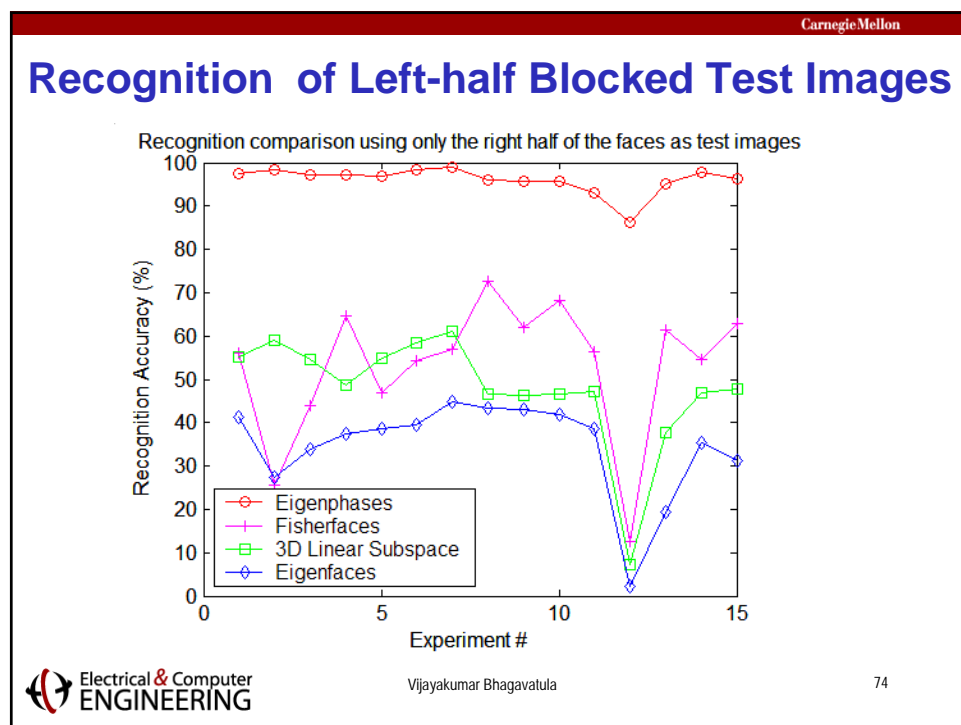
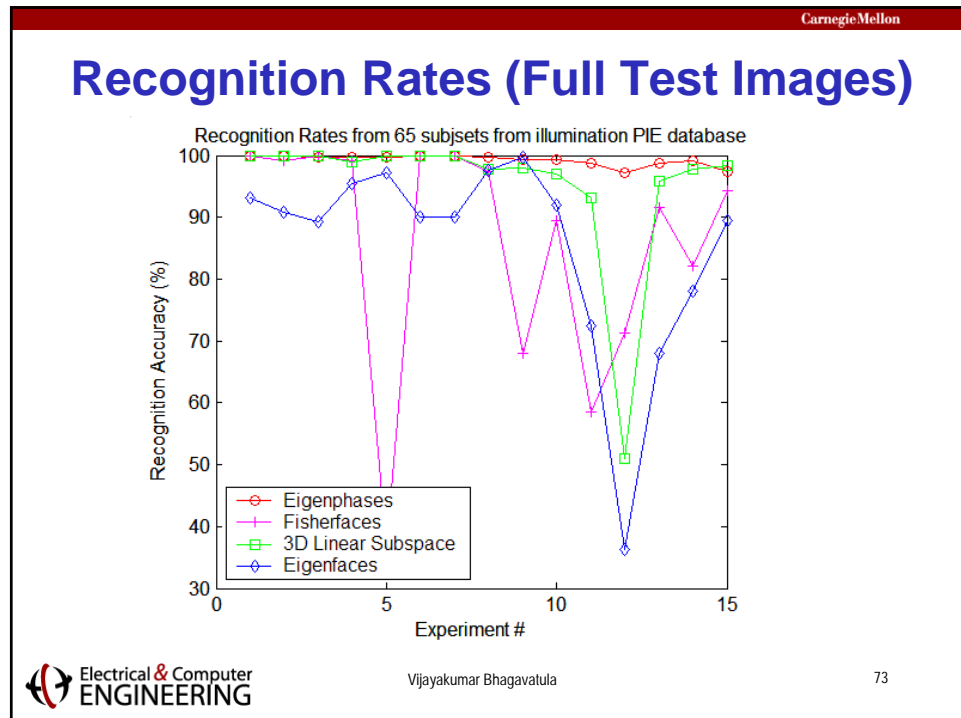
Electrical & Computer
ENGINEERING

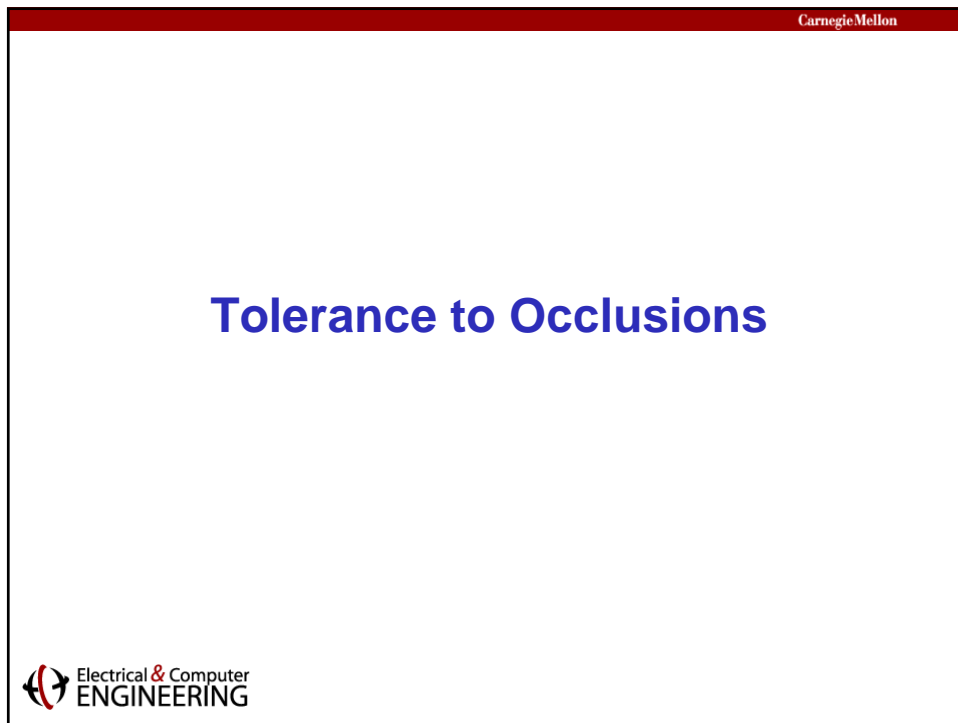
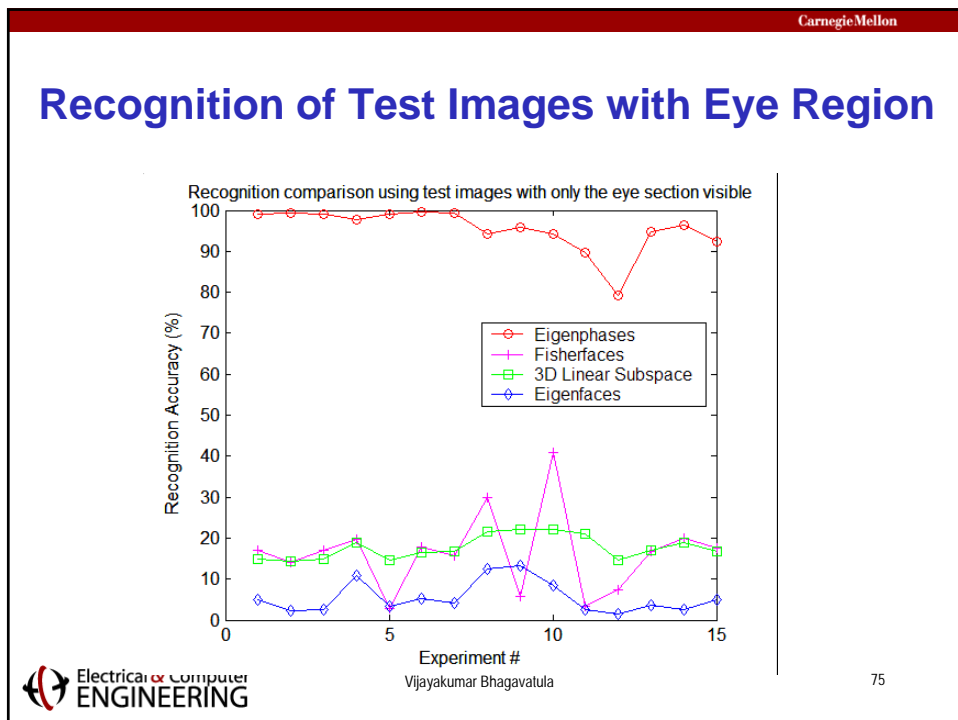
Test Images

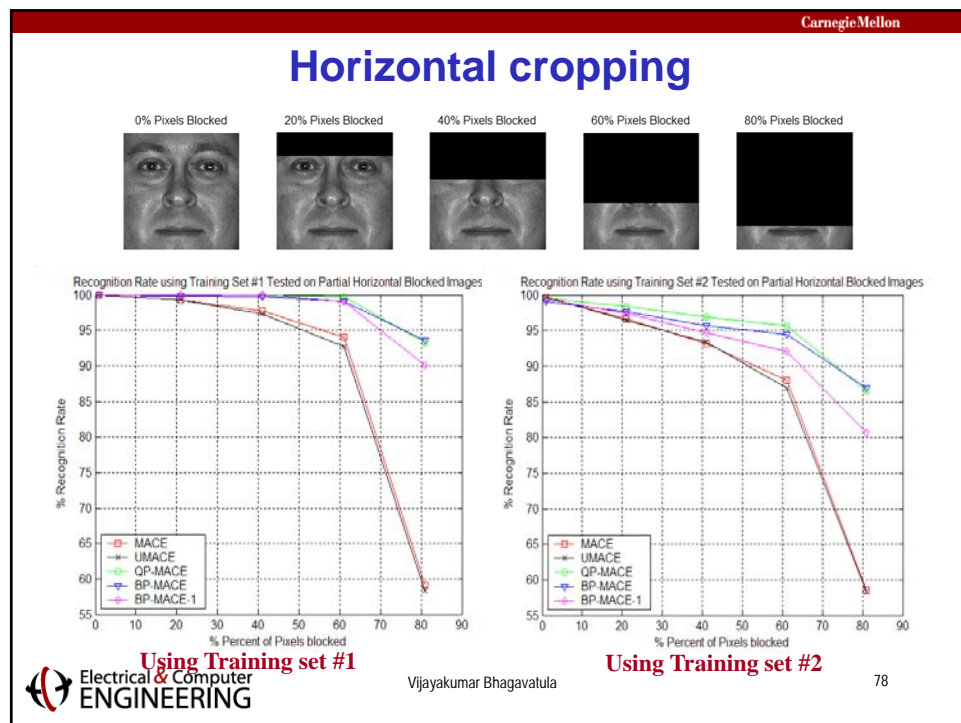
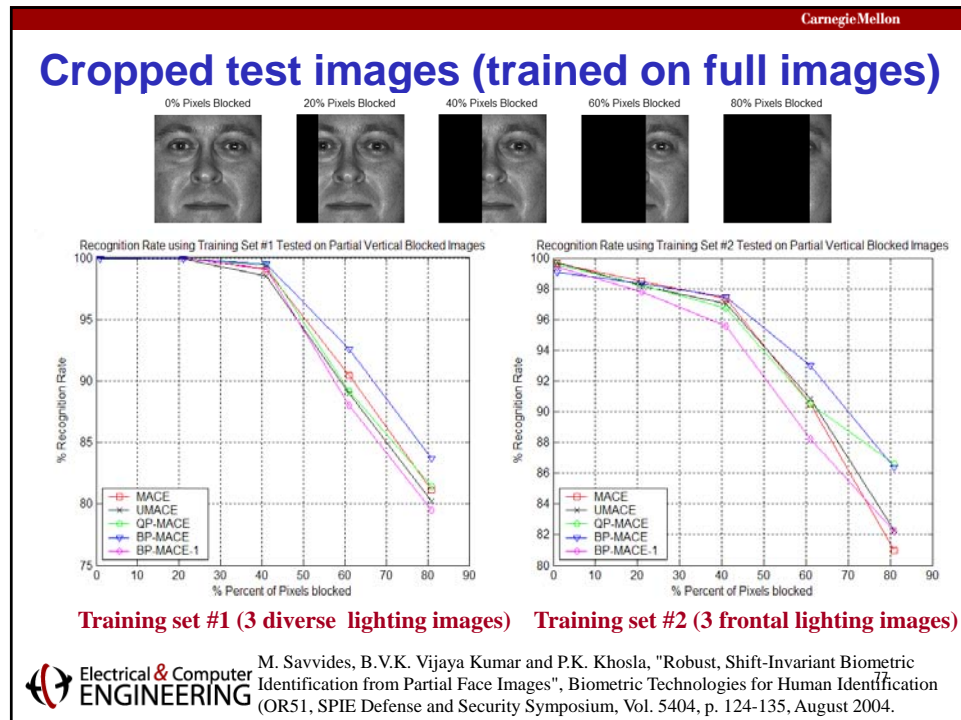
Training Images used were full images

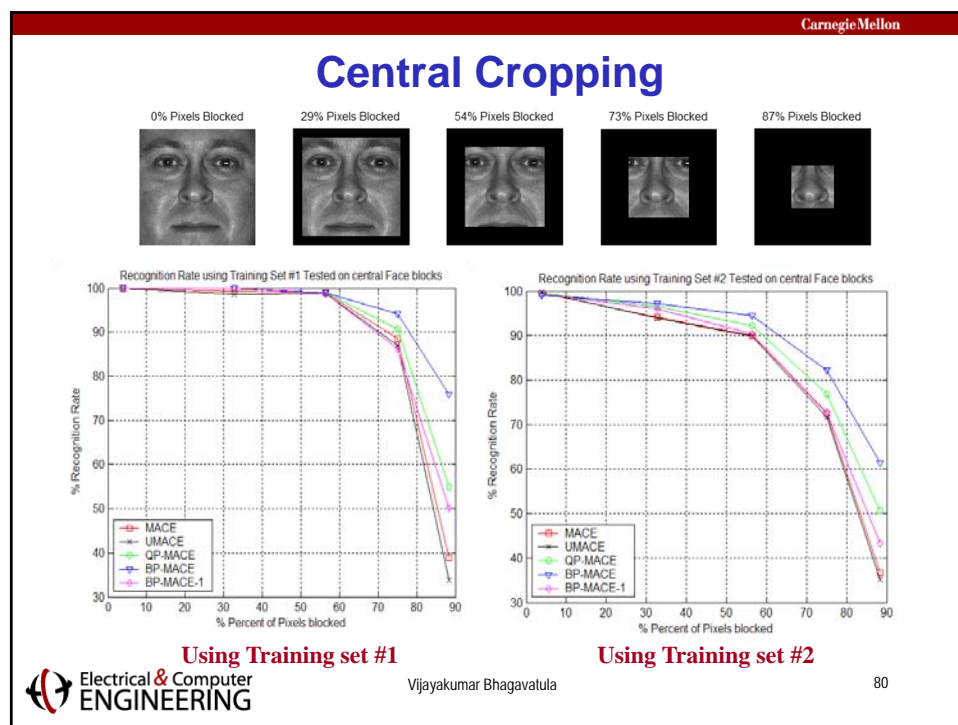
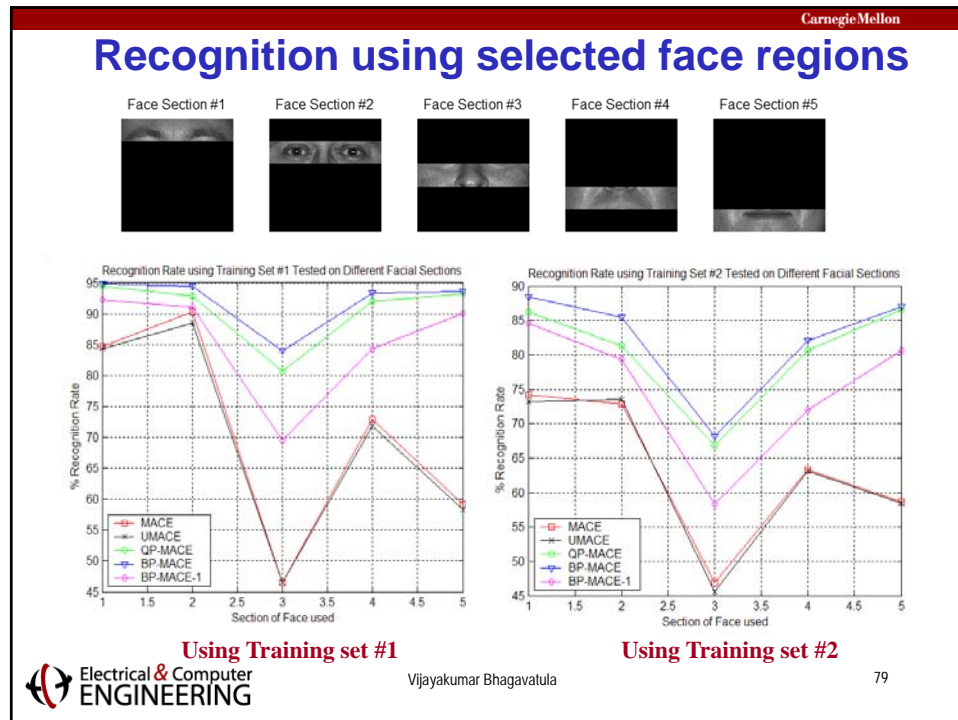


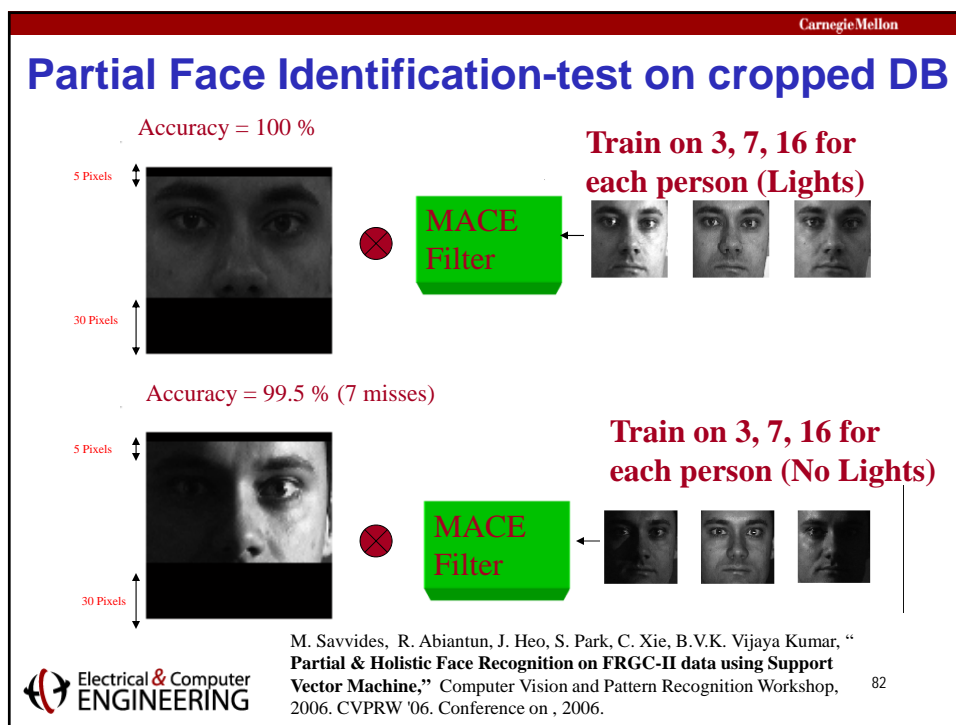
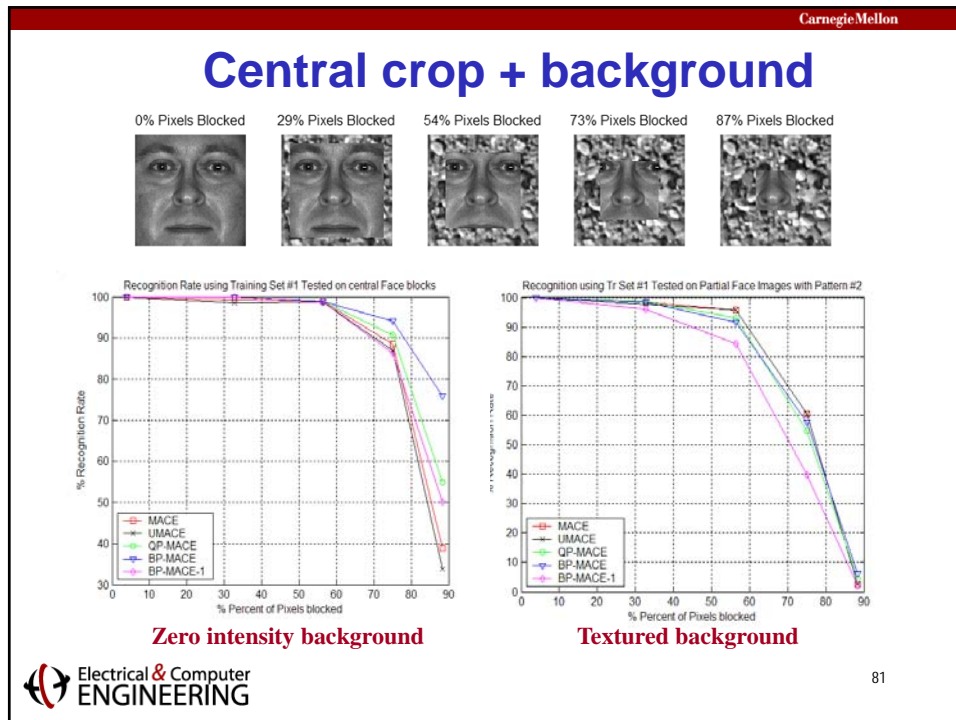
Electrical & Computer
ENGINEERING











Unconstrained MACE (UMACE) filter

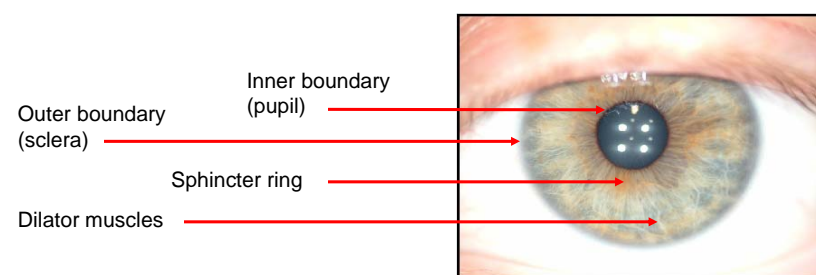
- UMACE Filter is similar to MACE except peak values are not constrained to yield a specific value
- Maximize average peak height $|\mathbf{h}^* \mathbf{m}|^2$, while minimizing average correlation energy ($\mathbf{h}^* \mathbf{D} \mathbf{h}$) leads to $\mathbf{h} = \mathbf{D}^{-1} \mathbf{m}$
- \mathbf{D} is a diagonal matrix containing average power spectrum of the training images
- \mathbf{m} is column vector containing the 2D Fourier transform of the average training image
- UMACE filter is simpler as it does not require matrix inversion
- Similarly, unconstrained OTSDF (UOTSDF) is given by $\mathbf{h} = \mathbf{T}^{-1} \mathbf{m}$ where $\mathbf{T} = \alpha \mathbf{D} + \sqrt{1 - \alpha^2} \mathbf{P}, \quad 0 \leq \alpha \leq 1$

Iris Recognition using Correlation Filters

Carnegie Mellon

Iris Biometric

Pattern source: muscle ligaments (sphincter, dilator), and connective tissue



The diagram illustrates the structure of the iris. It shows the outer boundary (sclera) in red, the inner boundary (pupil) in red, the sphincter ring in red, and the dilator muscles in red. The iris itself is shown in shades of brown and tan.

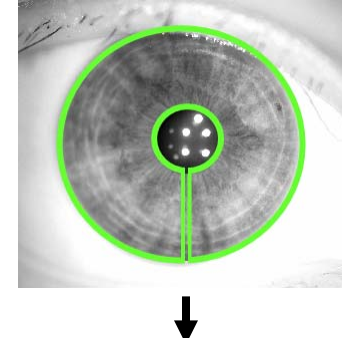
Outer boundary (sclera)
Inner boundary (pupil)
Sphincter ring
Dilator muscles

 Electrical & Computer
ENGINEERING

Carnegie Mellon

Iris Segmentation

“Unwrapping” the iris



The diagram shows a grayscale image of an iris being unwrapped from its circular form into a horizontal strip. A green circle highlights the outer boundary of the iris, and a green dot marks the center of the pupil.

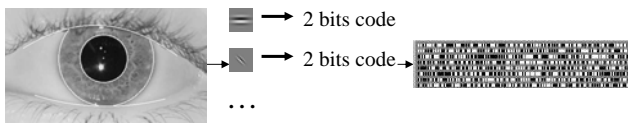
Outer boundary (with sclera)

Inner boundary (with pupil)

 Electrical & Computer
ENGINEERING

Carnegie Mellon

Daugman's Iris Recognition Method



Circular Edge Detector *Gabor Wavelet Analysis* *2048 bits iris code*

...

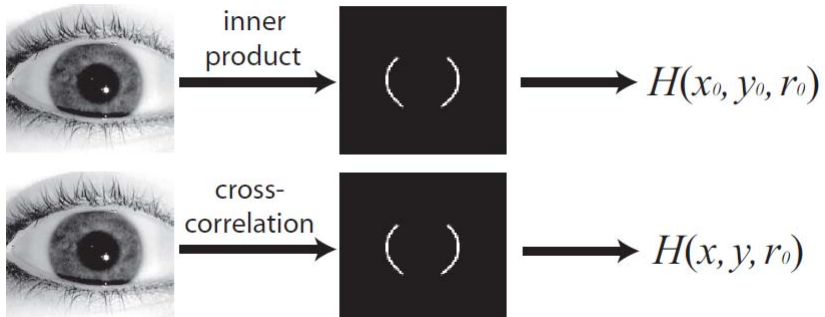
J. G. Daugman, "High confidence visual recognition of persons by a test of statistical independence,"
IEEE Trans. Pattern Anal. Machine Intell., Vol.15, pp. 1148-1161, 1993.

 Electrical & Computer
ENGINEERING

87

Carnegie Mellon

Matching the Contours

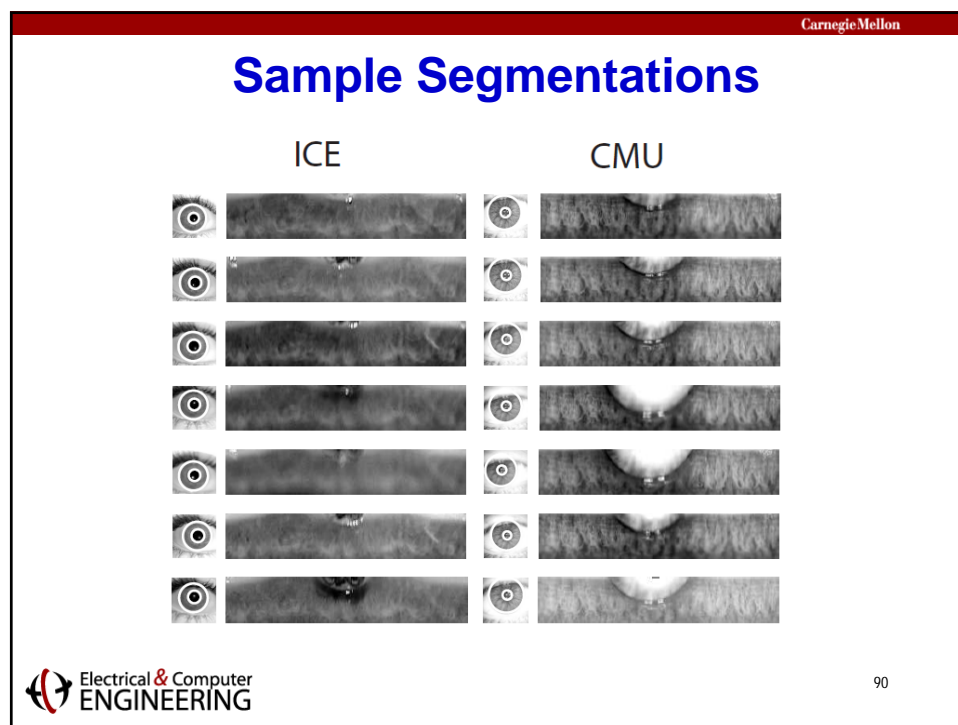
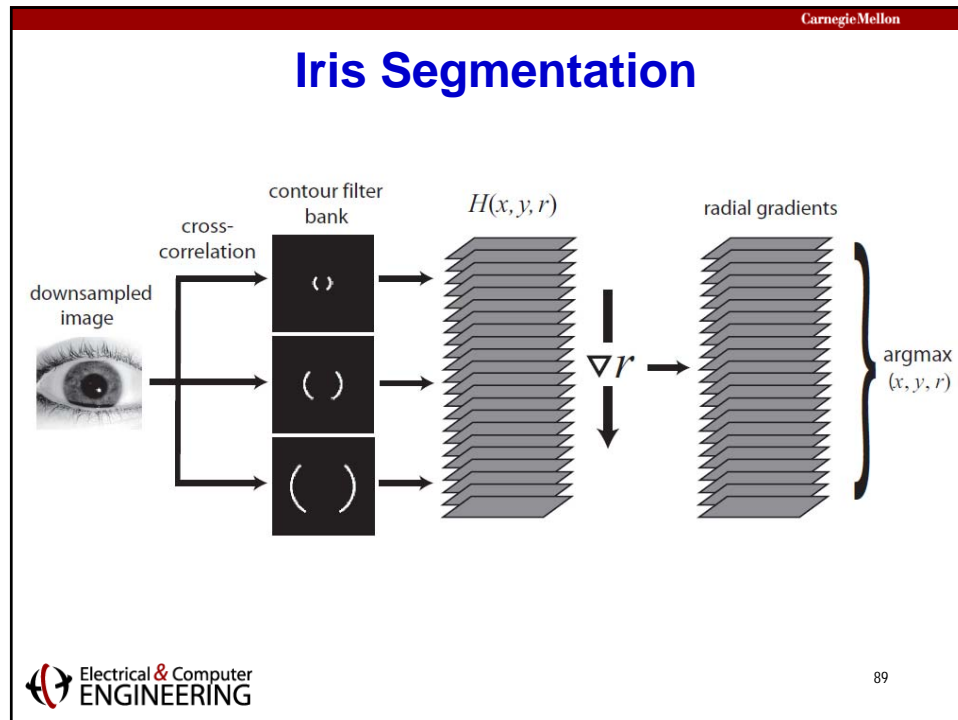


- ❑ Cross-correlation yields inner product of the contour template with the input image for all possible shifts
- ❑ Approximates circular Hough transform

J. Thornton, "Iris Pattern Matching: A Probabilistic Model based on Discriminative Cues," Ph.D. Dissertation, CMU, 2007.

 Electrical & Computer
ENGINEERING

88



Carnegie Mellon

Iris Recognition using Correlation Filters

We design a correlation filter for each iris class using a set of training images.

Determining an iris match with a correlation filter

J. Thornton, M. Savvides and B.V.K. Vijaya Kumar, "A unified Bayesian approach to deformed pattern matching of iris images," *IEEE Trans. Patt. Anal. Mach. Intell.*, vol. 29, 596-606, 2007.

Electrical & Computer
ENGINEERING

Carnegie Mellon

Iris Pattern Deformation

- Landmark points for all images within one class

Clear deformation from:

- Tissue changes AND/OR
- Deviations in iris boundaries.

Electrical & Computer
ENGINEERING

Eyelid Occlusion

Example : Eyelid artifacts in segmented pattern.



Example: match comparison

For significant portion of area, similarity is lost.



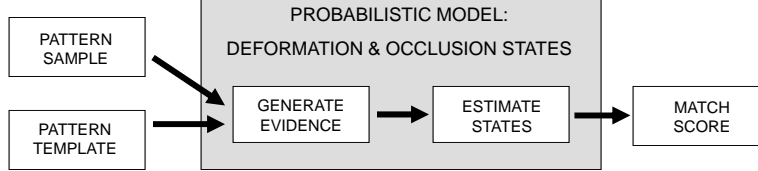
Iris Matching Approach

Goal: Accurate pattern matching when patterns experience

- relative nonlinear **deformations**
- partial **occlusions**

in addition to blurring and observation noise.

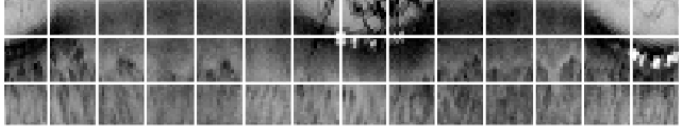
Approach



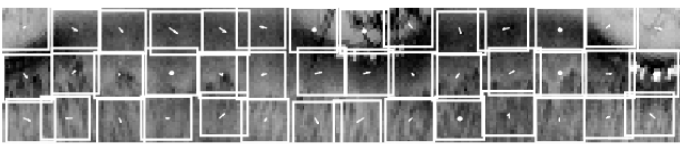
Carnegie Mellon

Hidden Variables: Deformation

Iris plane partitioned into 2D field:



Deformation described by vector field: $(\Delta x_i, \Delta y_i)$ for $(x, y) \in R_i$



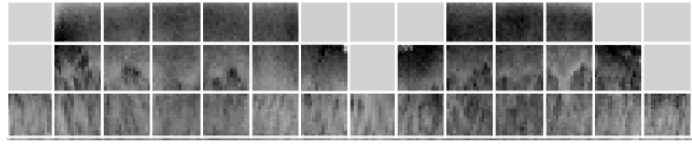
J. Thornton, M. Savvides and B.V.K. Vijaya Kumar, "A unified Bayesian approach to deformed pattern matching of iris images," *IEEE Trans. Patt. Anal. Mach. Intell.*, vol. 29, 596-606, 2007.

 Electrical & Computer
ENGINEERING

Carnegie Mellon

Hidden Variables: Occlusion

Occlusion described by binary field: $\lambda_i = \begin{cases} 1 & \text{if } R_i \text{ is occluded} \\ 0 & \text{if } R_i \text{ is unoccluded} \end{cases}$



Hidden vars: $H \triangleq \{ \Delta x_1, \Delta y_1, \lambda_1, \Delta x_2, \Delta y_2, \lambda_2, \dots \Delta x_N, \Delta y_N, \lambda_N \}$

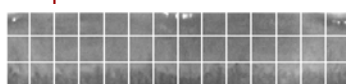
 Electrical & Computer
ENGINEERING

Role of Correlation Filters in Iris Matching

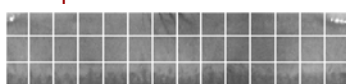
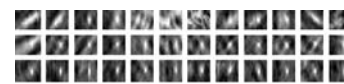
- ❑ Correlation filters used to compare a patch from the query to the corresponding patch from the reference
- ❑ Correlation peak provides a measure of the patch similarity
- ❑ Correlation peak location provides an estimate of the relative shift between the two patches
- ❑ These patch-based correlation outputs used as clues to infer the hidden variables (eyelid occlusions and local deformations)

Iris Matching Process

Template



New pattern

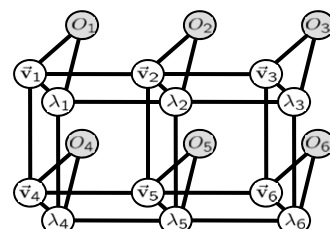
Similarity evidence $\{C_i(x, y)\}$ 

Eyelid evidence

 $\pi_1, \pi_2, \dots, \pi_N$

Goal : Infer posterior distribution on hidden states: $P(H|O)$

Inference technique : Loopy belief propagation



Carnegie Mellon

Iris Challenge Evaluation (ICE) 2005

Define Experiments

Exp 1

Right Eye



1425 Iris Images
124 Individuals

Exp 2

Left Eye



1528 Iris Images
120 Individuals

112 Overlapping Individuals
132 Total Individuals



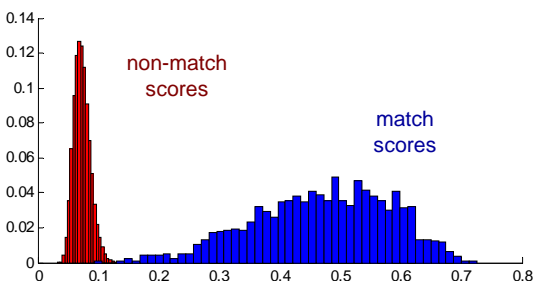
Source: Jonathon P. Phillips, NIST 99

 Elect. ENGINEERING

Carnegie Mellon

ICE 2005 Performance

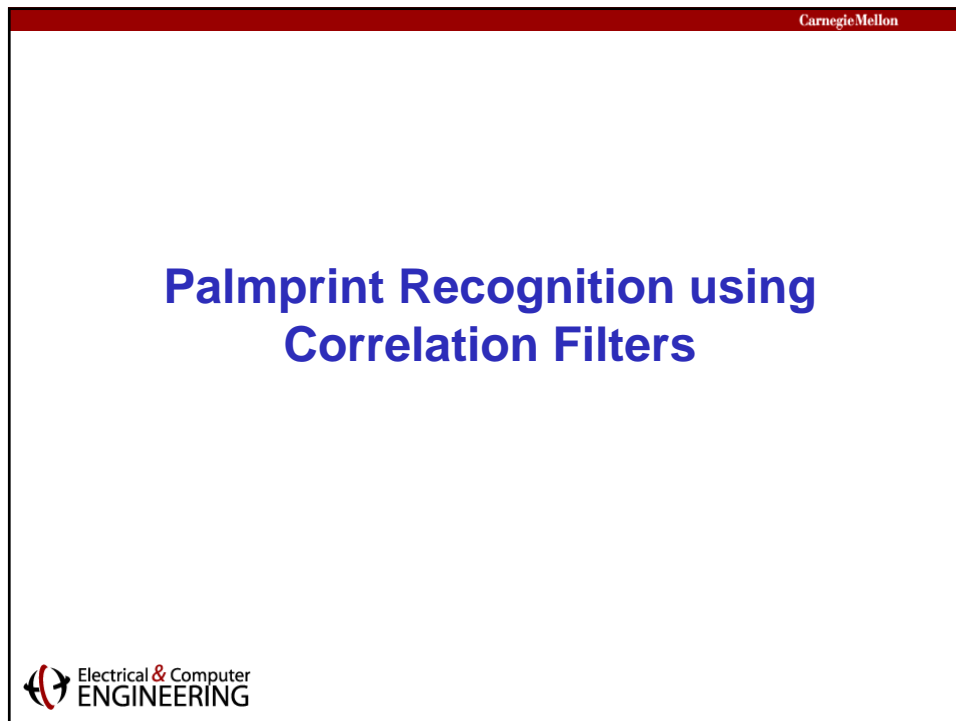
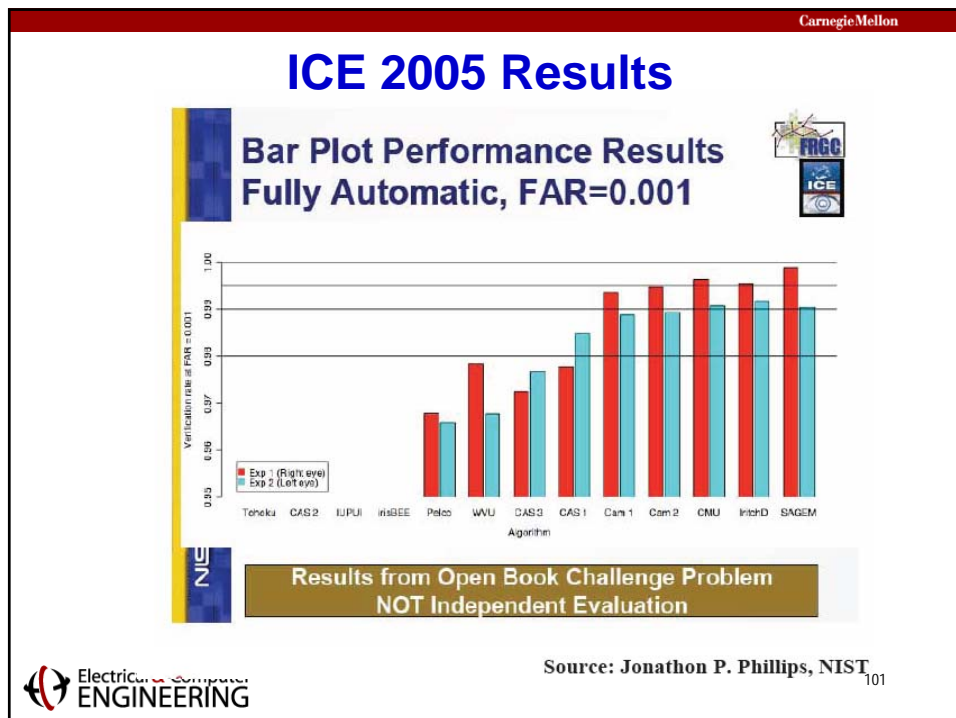
Experiment 1 score distribution



Verification Rate at FAR = 0.1%

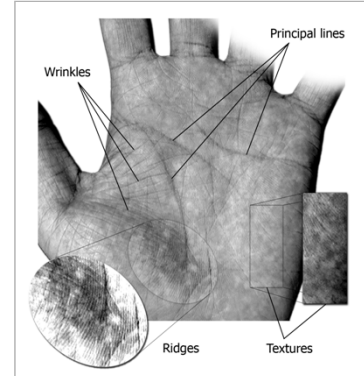
Experiment 1: 99.63 % Experiment 2: 99.04 %





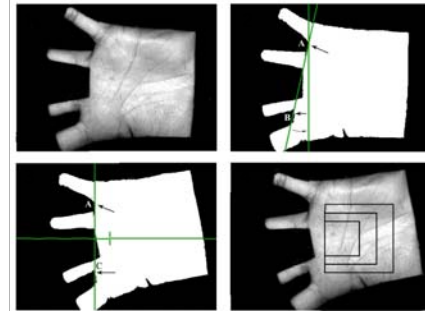
Palmprint Features

- ❑ Palmprints have a conglomerate of features.
- ❑ These include principal lines, smaller creases or wrinkles, fingerprint-like ridges and textures.
- ❑ Palmprints can be easily aligned about fiducial points of the hand's geometry or shape.



Palmprint Extraction

- ❑ First we find two fiducial points from the contour of the hand.
- ❑ We rotate the palm so that the points are aligned to the vertical axis.
- ❑ A region can be extracted using these points as a reference.



Carnegie Mellon

Palmprint Matching

- PolyU Palmprint Database
- 100 palms (classes)
- Left hands flipped to look as right hands
- 3 images per class for training
- 3 images per class for testing
- 5 different experiments using region sizes with sides of 64, 80, 96, 112, and 128 pixels

Left hand Left hand flipped Right hand

Vijayakumar Bhagavatula

105

 Electrical & Computer
ENGINEERING

Carnegie Mellon

Optimal Tradeoff Filter Performance

I

RESULTS OF OTSDF FILTER CLASSIFIER USING 100 CLASSES.

<i>n</i>	Avg FRRz (<i>M</i> ₁)	Avg FARz (<i>M</i> ₂)	Id Acc
64	2.6% (8)	0.07% (23)	97.3%
80	1.0% (3)	0.02% (6)	98.3%
96	0.3% (1)	0.01% (3)	98.6%
112	1.0% (3)	0.01% (3)	99.0%
128	0.3% (1)	0.03% (10)	99.6%

Avg FRRz: Average FRR at zero FAR. *M*₁ misses out of 300.
Avg FARz: Average FAR at zero FRR. *M*₂ misses out of 29, 700.
Id Acc: Identification Accuracy.

P. Hennings, B.V.K. Vijaya Kumar and M. Savvides, "Palmprint classification using multiple advanced correlation filters and palm-specific segmentation," *IEEE Trans. Information Forensics and Security*, vol. 2, 613-622, 2007.

 Electrical & Computer
ENGINEERING

Vijayakumar Bhagavatula

106

Eye Detection using Correlation Filters



Eye Detection

- ❑ Eye detection can be useful for inter-ocular distance-based geometric normalization of ocular images
- ❑ Viola and Jones eye detector perhaps the best known
- ❑ More recent work by Bolme using Average Synthetic Exact Filters (ASEFs, CVPR 2009) and Minimum Output Sum of Squared Error Filter (MOSSE, CVPR 2010) to locate eyes in face images
- ❑ We developed an improved correlation filter formulation called Max-Margin Correlation Filter (MMCF) and used it for eye detection

D. S. Bolme, B. A. Draper, and J. R. Beveridge, "Average of Synthetic Exact Filters," Computer Vision and Pattern Recognition. 2009.

D. S. Bolme, J. R. Beveridge, B. A. Draper, and Y. M. Lui, "Visual Object Tracking using Adaptive Correlation Filters," Computer Vision and Pattern Recognition. 2010.



Eye Detection Experiments

- ❑ FERET database (Phillips et al., IEEE T-PAMI, 2000)
- ❑ OpenCV face detector used to extract 128x128 images with eyes at pixel locations (32,40) and (96,40)
- ❑ To make the eye detection challenging, we applied a random similarity transform with translation of up to +/- 4 pixels, scale up to +/- 10% and rotations up to +/- $\pi/16$ radians
- ❑ 3400 images of 1204 people
- ❑ We randomly partitioned the dataset with 512 images used for training, 675 for parameter selection by cross-validation and the rest for testing

Example Correlation Outputs



Probe Image

Right Eye
Correlation
OutputLeft Eye
Correlation
Output

Eye Detection Results

- Accuracy of eye location quantified by $D = \frac{\|P - \hat{P}\|}{\|P_l - P_r\|}$
- P is the ground truth location, \hat{P} is the predicted location
- P_l and P_r are the true locations of the left and the right eye
- Localization (i.e., $D < 0.1$) performance results averaged over 5 different runs with random partitions for training and testing and random similarity transforms

Eye	ASEF	MOSSE	MMCF
Left	91.2	94.1	95.1
Right	90.6	92.9	93.6

- Our results for ASEF and MOSSE are consistent with those reported by Bolme for the same task
- MMCF outperforms ASEF and MOSSE in eye location task

Ocular Recognition using Correlation Filters

Carnegie Mellon

Challenging Ocular Image Recognition (COIR)

- ❑ **Ocular recognition:** use iris regions as well as periocular regions to achieve improved matching
- ❑ **Goal:** to improve the matching of the ocular images in challenging acquisition conditions (occlusions, eye gaze angle differences, low spatial resolution, shadows, different spectral bands (RGB, near-IR), etc.)



Shadow



Low Resolution



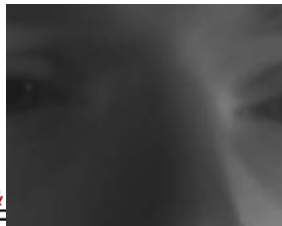
Color Iris Image

Face and Ocular Challenge Series (FOCS) Dataset

- ❑ Images were captured from moving subjects, in an unconstrained environment.
- ❑ Number of images: 9588
- ❑ Resolution of images: 750 x 600
- ❑ Number of subjects: 136
- ❑ Number of samples per subject
 - Not consistent. Varies from 2 ~ 236 samples/subject
 - Mean: 70
 - Median: 59
 - 123 subjects have more than 10 samples each

Carnegie Mellon

FOCS: Challenges

Occlusion	Off-angle Gaze
	
Movement	Illumination
	

 Electrical &
ENGINEERING

Vijayakumar Bhagavatula

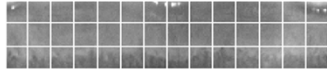
115

Carnegie Mellon

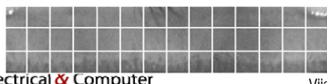
Probabilistic Deformation Model

- ❑ Probabilistic deformation models (PDMs) for improved iris/ocular matching
 - ❑ By segmenting the template and query images into patches we can measure the relative deformation through cross correlation.
 - ❑ MAP estimation is then implemented to maximize the posterior probability distribution on latent deformation variables. Effectively learning the proper ‘movements’ for similar patterns to assign a higher match score, while uncorrelated query images will exhibit seemingly random ‘movements’ giving them a lower match score.

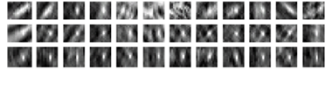
Template



New pattern



Similarity evidence $\{C_i(x, y)\}$

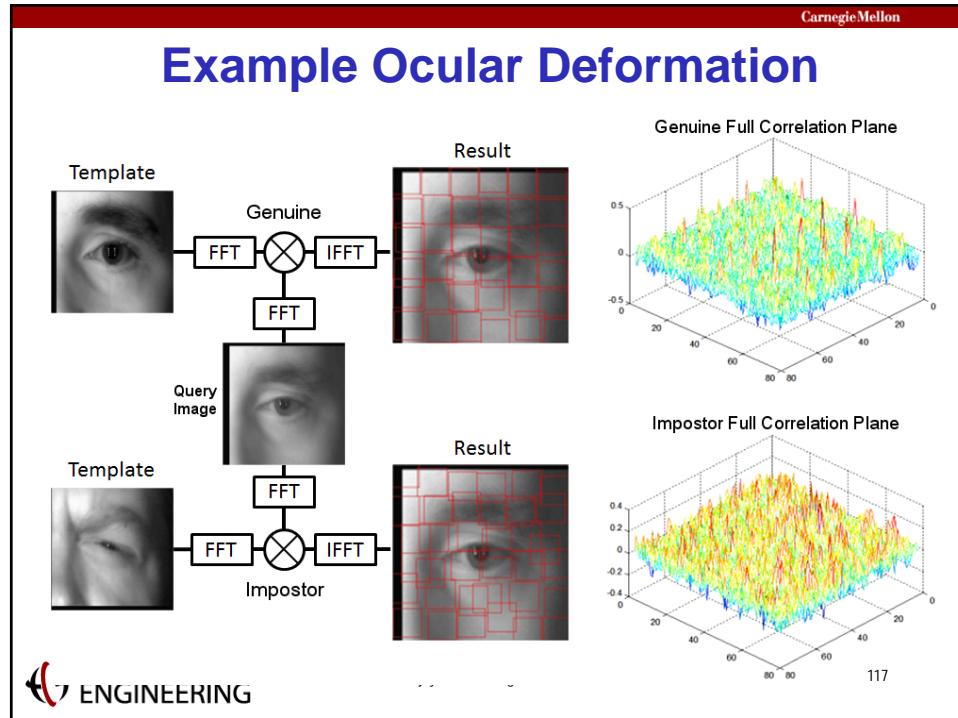


Eyelid evidence
 $\pi_1, \pi_2, \dots, \pi_N$

 Electrical & Computer
ENGINEERING

Vijayakumar Bhagavatula

116



Carnegie Mellon

Performance of Ocular Recognition Approaches

	Left-with-left		Right-with-right	
	EER	FRR	EER	FRR
PDM	23.4%	58.5%	23.9%	61.4%
GOH	32.9%	97.4%	33.2%	97.0%
m-SIFT	28.8%	67.8%	27.2%	65.9%
Iris	33.1%	81.3%	35.2%	81.2%

FRR at 0.1% FAR

Vishnu Naresh Boddeti, Jonathon Smereka and B.V.K. Vijaya Kumar, "A comparative evaluation of iris and ocular recognition methods on challenging ocular images," *Intl. Joint Conference on Biometrics (IJCB)*, October 2011.

Electrical & Computer
ENGINEERING

Vijayakumar Bhagavatula

118

Carnegie Mellon

Fusion Performance

	Left-with-left		Right-with-right	
	EER	FRR	EER	FRR
PDM+GOH	19.5%	71.7%	19.4%	70.1%
PDM+m-SIFT	23.9%	57.6%	23.3%	60.0%
GOH+m-SIFT	31.2%	96.2%	27.2%	95.5%
PDM+GOH+m-SIFT	19.3%	70.5%	19.3%	68.8%
(0.1*PDM)+(0.1*GOH)+(0.8*m-SIFT)	18.8%	63.8%	18.8%	61.4%
(0.75*PDM)+(0.15*GOH)+(0.10*m-SIFT)	21.7%	55.4%	21.2%	58.0%

❑ Best FRR at 0.1% FAR is 55.4%

❑ **Best EER is 18.8%**

R. Jillella, A. Ross, V.N. Boddeti, J. Smereka, B.V.K. Vijaya Kumar and V. Paul Pauca, "Matching highly nonideal ocular images: An information fusion approach," *International Conference on Biometrics (ICB)*, New Delhi, India, March 2012.



Vijayakumar Bhagavatula

119

Carnegie Mellon

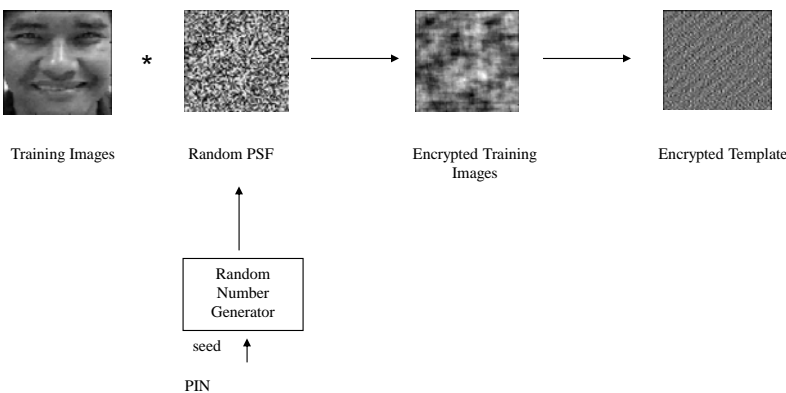
Cancelable Correlation Filters



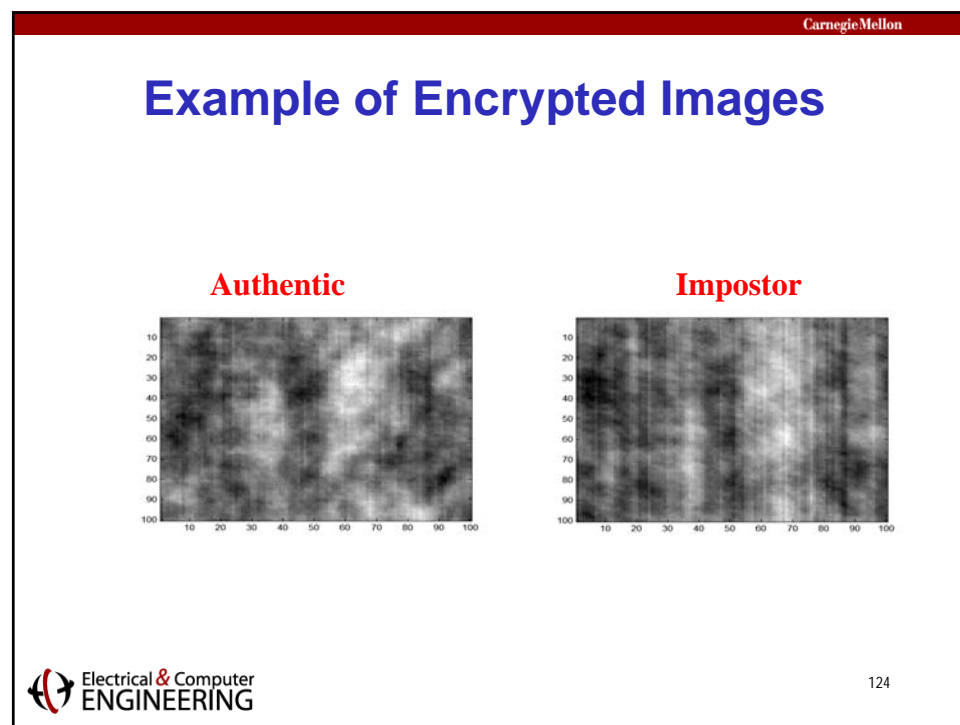
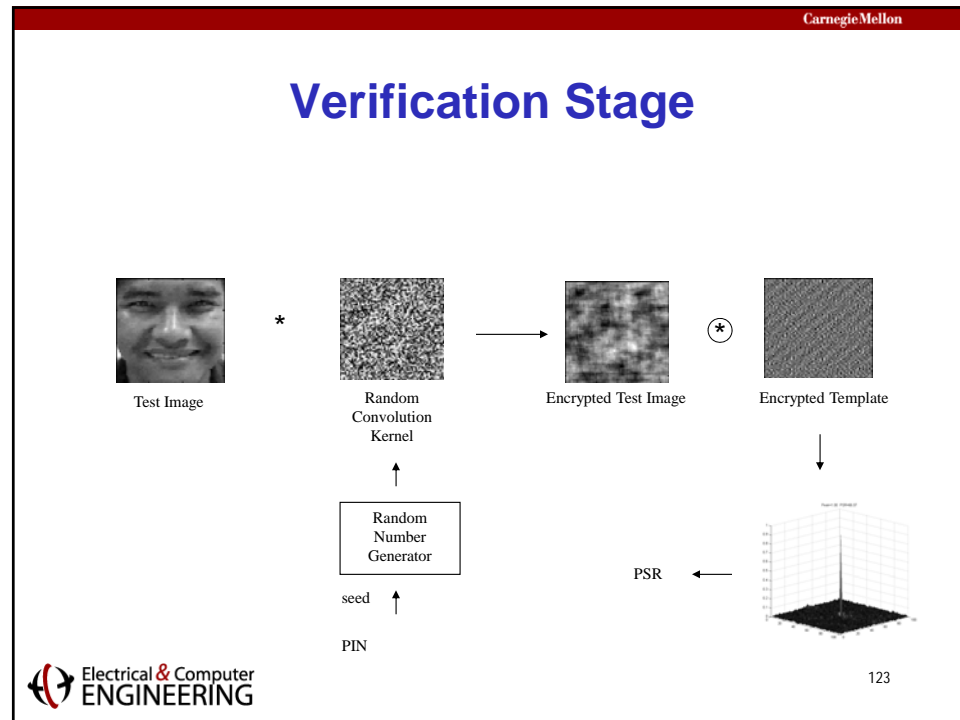
Cancellable Biometric Filters

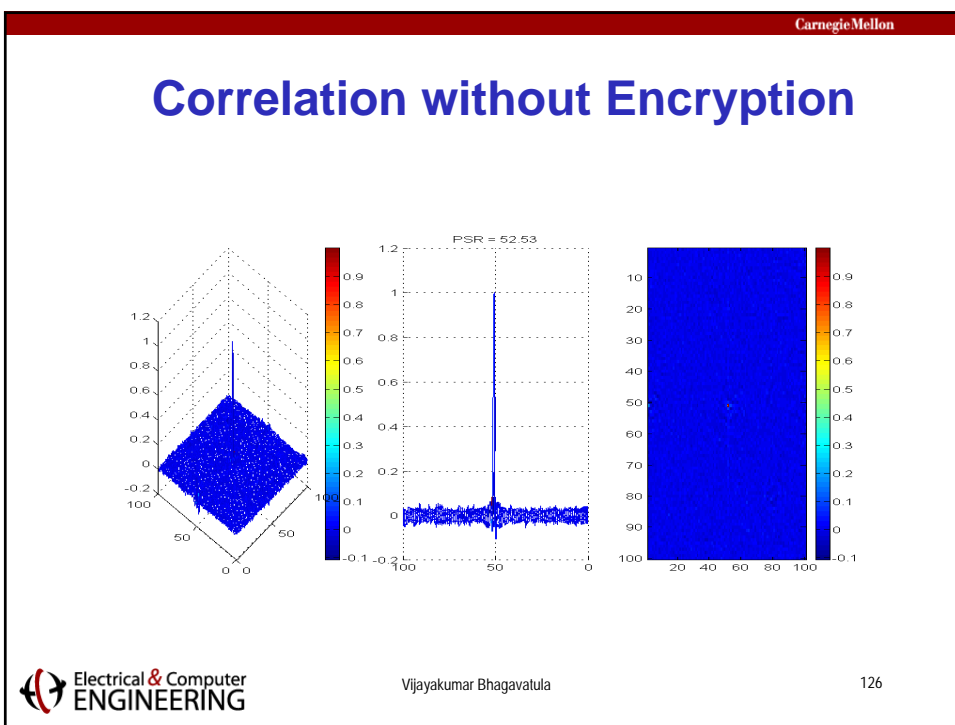
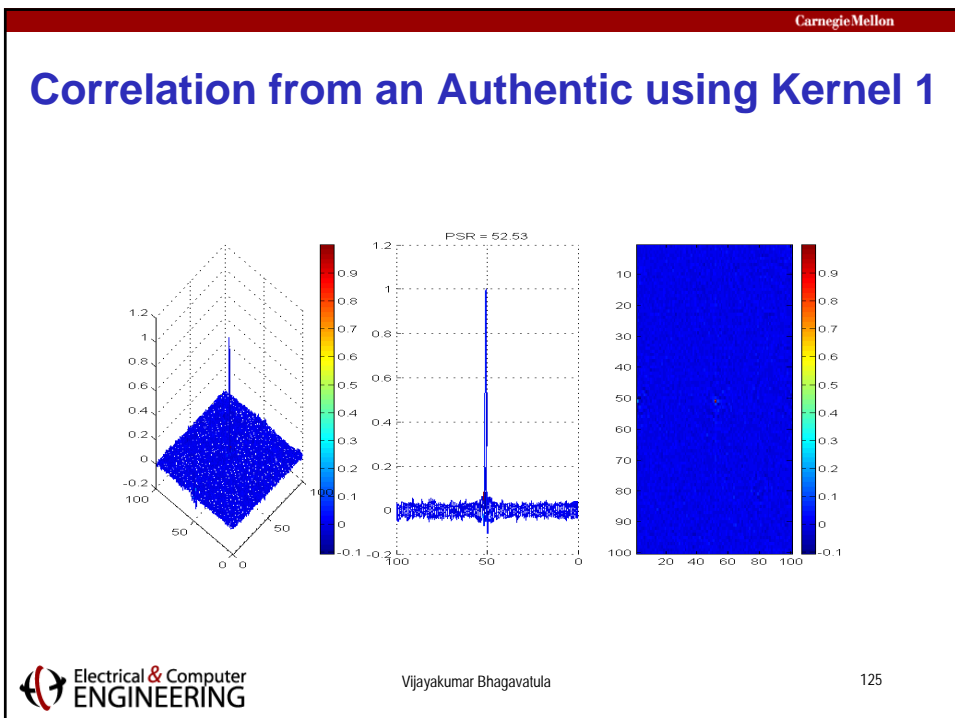
- ❑ A biometric filter (stored on a card) can be lost or stolen
 - Can we reissue a different one (just as we reissue a different credit card)?
 - There are only a limited set of biometric images per person (e.g., only one face)
- ❑ A new correlation filter can be constructed from the same biometric

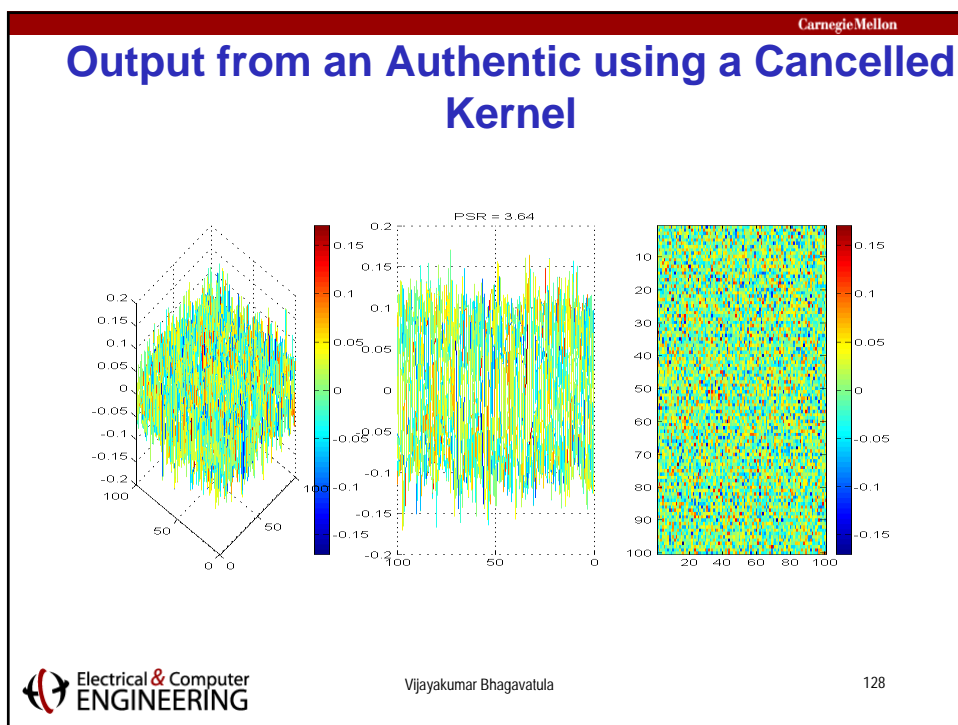
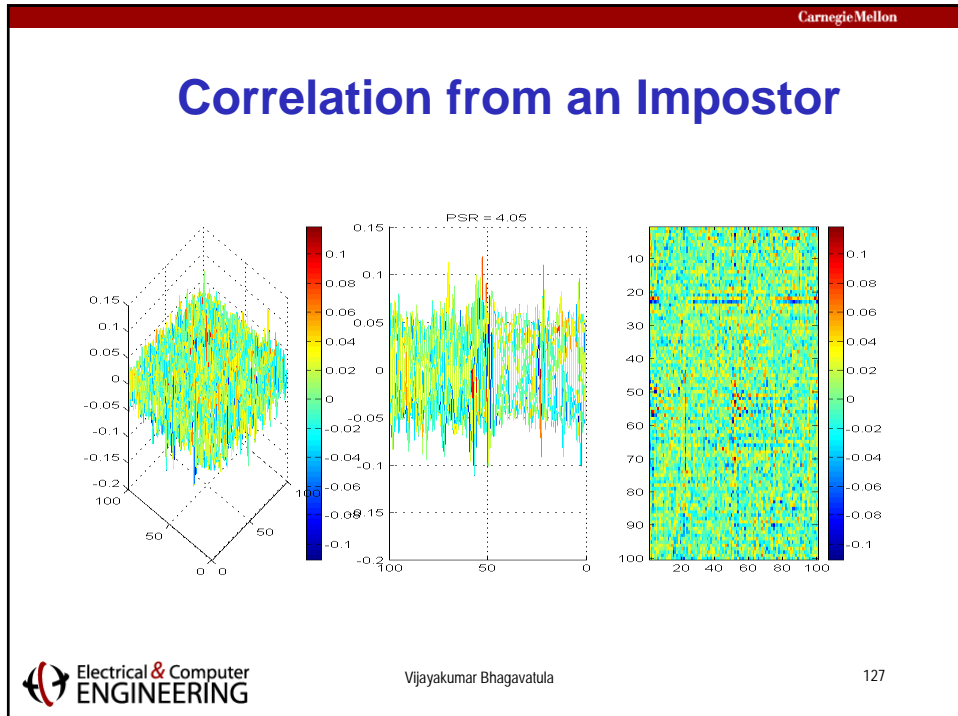
Enrollment Stage



M. Savvides and B.V.K. Vijaya Kumar, "Cancelable biometric filters for face recognition," *Intl. Conf. on Pattern Recognition (ICPR)*, 922-925, 2004.



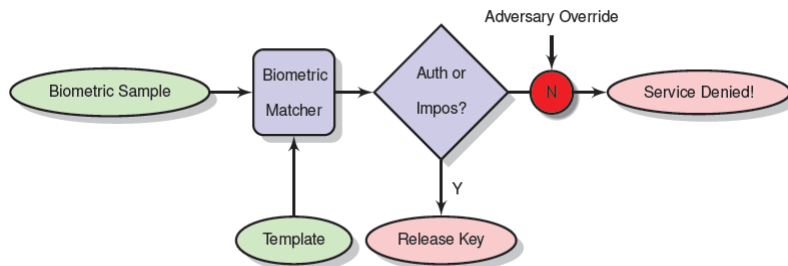




Biometric Encryption



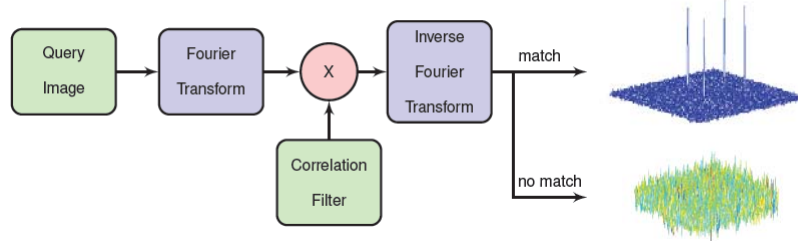
Key Extraction from Biometric Authentication



- Problem: Attacker can substitute the matching decision from the biometric authentication system



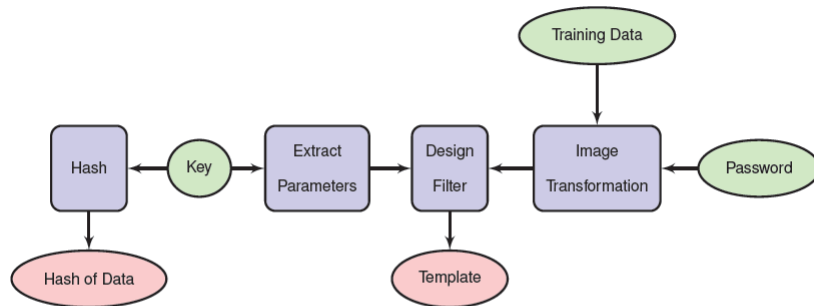
Multi-peak Correlation Filters



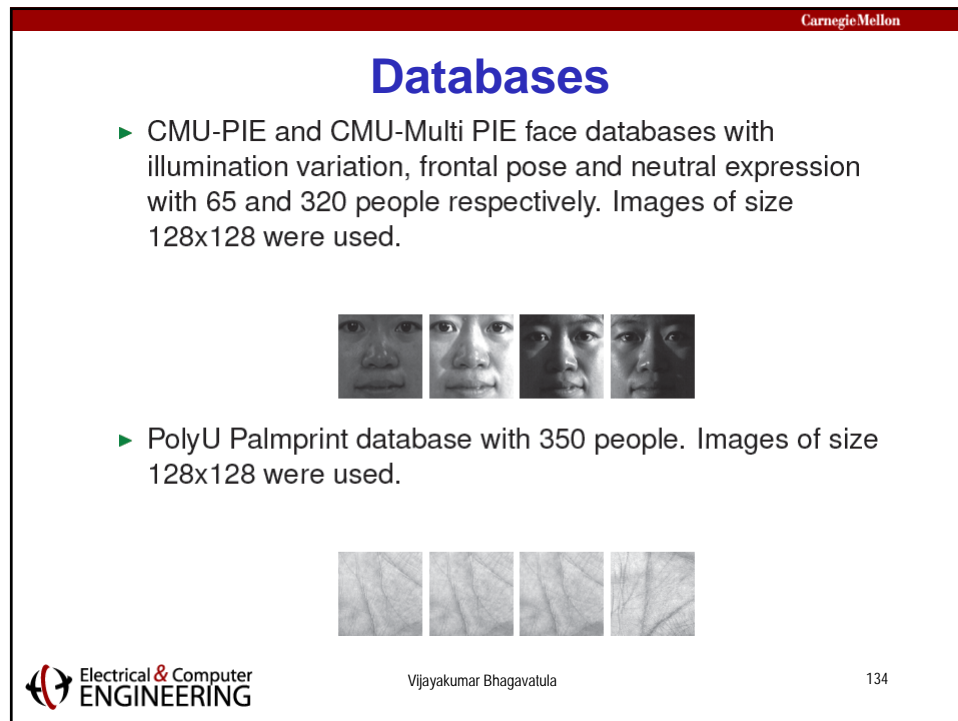
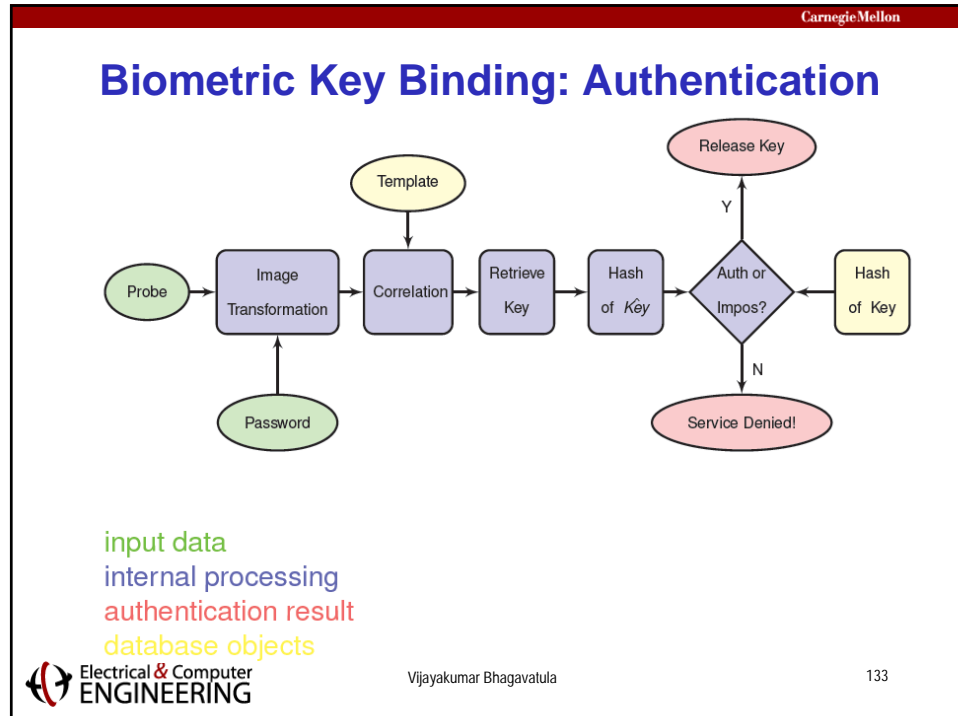
- The (x,y) coordinates of correlation output peaks contain the secret key for that person

Vishnu Naresh Boddegi, F. Su and B.V.K. Vijaya Kumar, "A biometric key-binding and template protection framework using correlation filters," *Intl. Conf. on Biometrics (ICB)*, 2009.

Biometric Key Binding: Enrollment



input data
internal processing
enrollment data stored in secure database



Single User Key-binding

Key Retrieval Failure Percentages

Key Size (bits)	Brute Force Security (bits)	Lights	Nolights	MPIE	Palmprint
64	58	0.0	0.0	0.1	0.5
128	112	0.0	0.0	0.2	1.2
256	231	0.0	0.0	0.6	3.0
512	451	0.0	4.3	6.0	11.7
770	671	0.7	20.3	18.9	24.1

- Impostor key retrieval rate is zero in all experiments

Single User Multi-biometric Key-binding

Key Retrieval Failure Percentages

Key Size (bits)	Brute Force Security (bits)	Lights + Palm	Nolights + Palm
64	58	0.0	0.0
128	112	0.2	0.2
256	231	0.0	0.2
512	451	0.5	1.8
800	695	1.3	4.7

Multi-user Key-binding

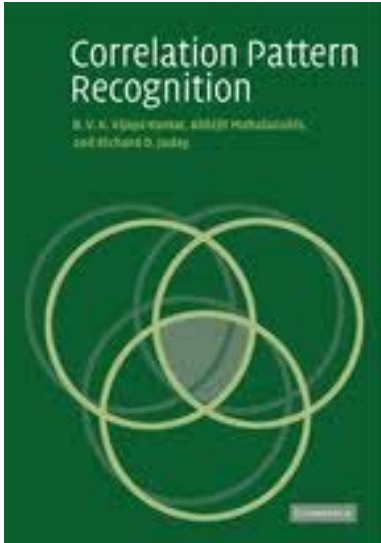
Key Retrieval Failure Percentages

Key Size (bits)	Brute Force Security (bits)	Lights	Nolights
64	58	0.0	0.0
128	112	0.0	0.0
256	231	0.0	0.0
512	451	0.0	1.0
800	695	0.0	2.4

Summary

- ❑ Correlation filters
 - Exhibit excellent performance on face recognition grand challenge (FRGC) images
 - Performed well in iris challenge evaluation (ICE)
 - Performed well on challenging ocular image recognition
 - Enable the design of cancelable biometric templates
 - Enable the binding of secret keys to biometrics
- ❑ Correlation filters provide a single matching engine for a variety of image biometrics tasks
- ❑ While frequency-domain representations are not intuitive, they can be highly beneficial

Carnegie Mellon



**Correlation Pattern
Recognition**
B.V.K. Vijaya Kumar, A. Mahalanobis,
& Richard D. Juday

Table of Contents

- 1. Introduction
- 2. Mathematical background
- 3. Linear systems and filtering theory
- 4. Detection and estimation
- 5. Correlation filter basics
- 6. Advanced correlation filters
- 7. Optical considerations
- 8. Limited-modulation filters
- 9. Applications of correlation filters
- References

139

 Electrical & Computer
ENGINEERING